CSIC
Consejo Superior de Investigaciones Científicas
Vniversitat de València
IFIC Institut de Física Corpuscular
Excelencia Severo Ochoa

Based on **Barbieri+** (2602.11100)
Accepted for publication in JCAP

In collaboration with L. Caloni,
M. Gerbino, M. Lattanzi and L. Visinelli

Precise cosmological bounds on Axion-Like Particles

NICOLA BARBIERI – IFIC (CSIC-UV)

CMB search of relativistic species

[Bashinsky, Seljak: Phys. Rev. D 69 (2004) 083002]
[Hou et al: Phys. Rev. D 87 (2013) 083008]
[Follin et al: Phys. Rev. Lett. 115 (2015) 091301]
[Baumann et al: JCAP 01 (2016) 007]

- Additional energy density in neutrinos is accounted by assuming that they have a thermal distribution with an effective energy density

$$\rho_\nu = N_{\text{eff}} \times \frac{7}{8}\left(\frac{4}{11}\right)^{4/3} \rho_\gamma$$

Background: at fixed acoustic scale, an increase in the radiation energy density leads to enhanced damping at small scales

Perturbations: fluctuations in free-streaming radiation travel faster than the sound speed of the photon-baryon plasma. Thus, phase (and amplitude) shifts at small angular scales.

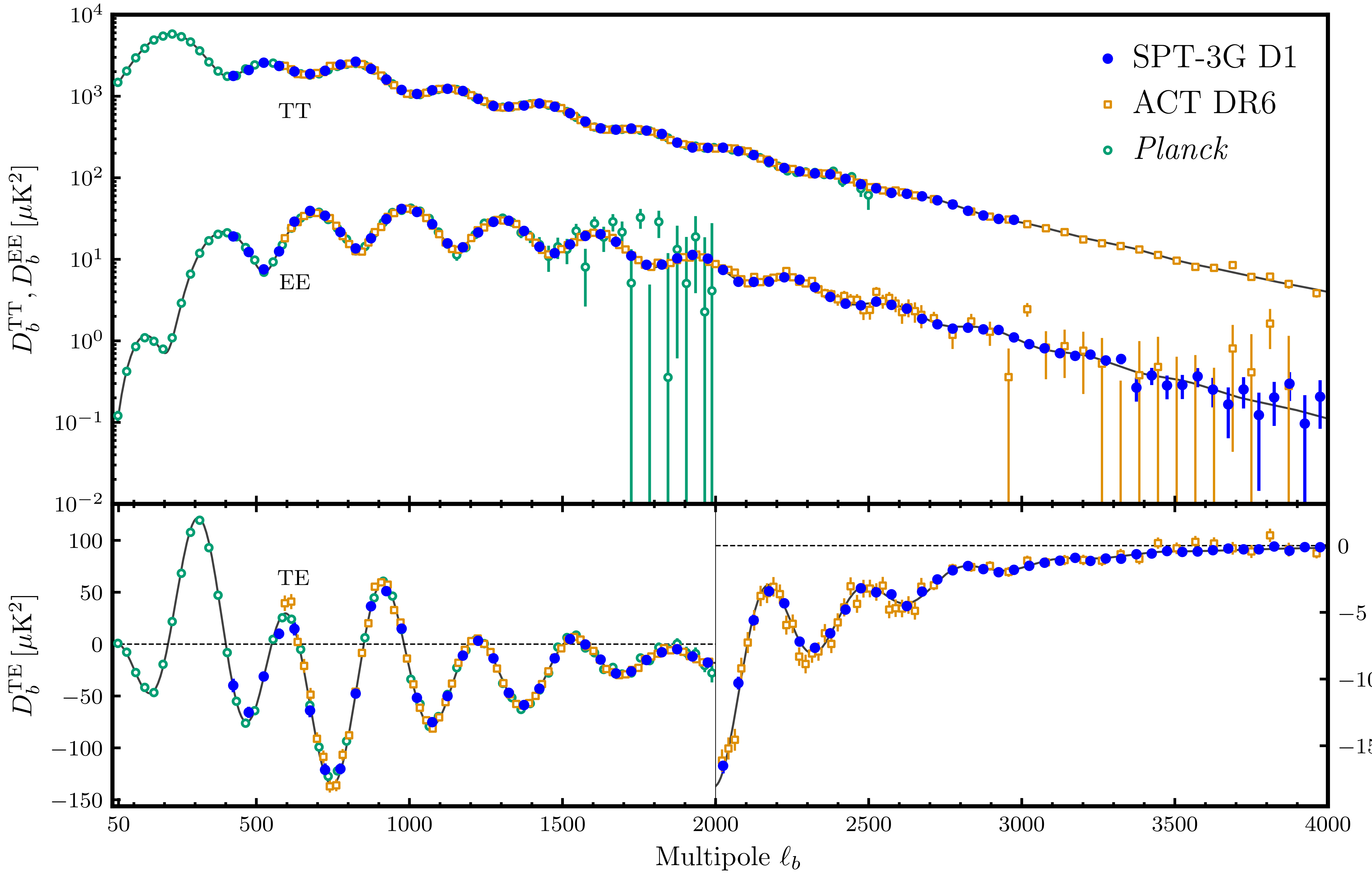

[Image credits: SPT Collaboration]

Cosmo-phenomenology of thermal axions

- The QCD axion is a pseudo Nambu-Goldstone boson (PNG) resulting from the SSB of a global U(1) symmetry, introduced to solve the strong CP problem of QCD.

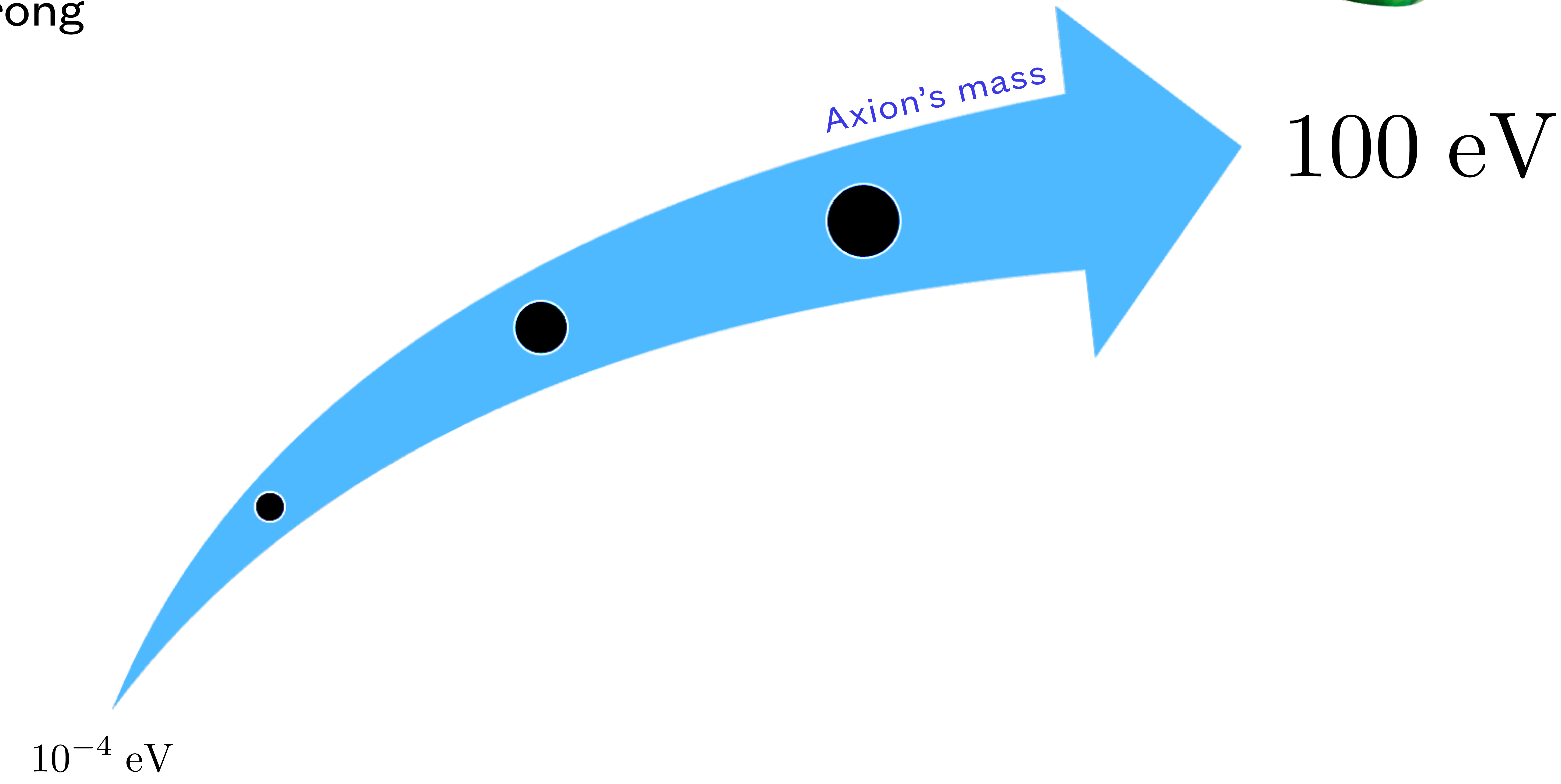

Cosmo-phenomenology of thermal axions

- The QCD axion is a pseudo Nambu-Goldstone boson (PNG) resulting from the SSB of a global U(1) symmetry, introduced to solve the strong CP problem of QCD.

$$\Delta N_{\mathrm{eff}} \equiv \frac{\rho_a\,(m_a = 0)}{\rho_{\nu,\mathrm{mless}}} \propto \left(\frac{g_a}{g_\gamma}\right)\left(\frac{T_a}{T_\gamma}\right)^4$$

$$\simeq 0.027 \left(\frac{g_{*s}\,(T_d)}{106.75}\right)^{-4/3}$$

Light axions contribute to the energy density of radiation

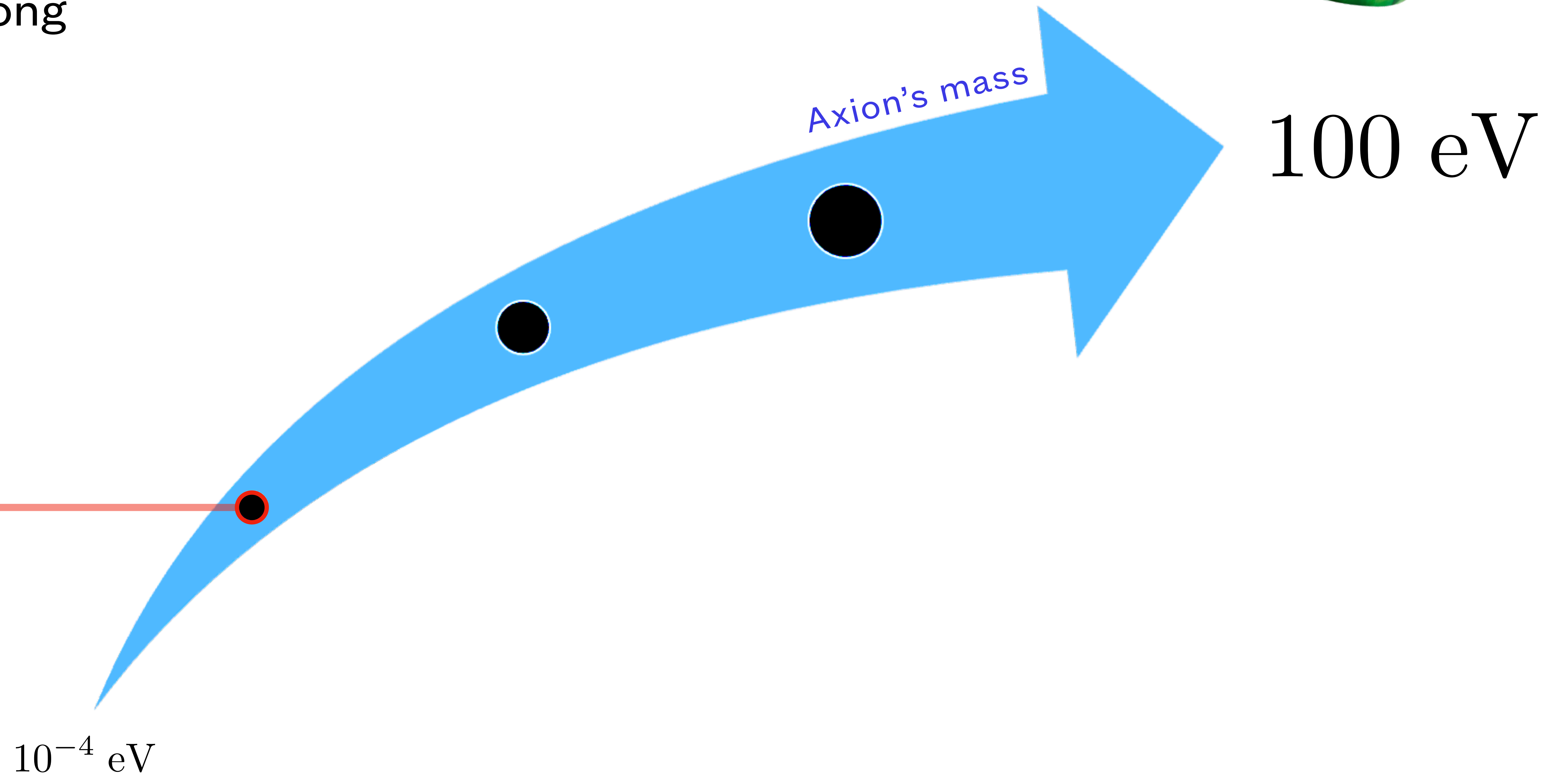

Cosmo-phenomenology of thermal axions

- The QCD axion is a pseudo Nambu-Goldstone boson (PNG) resulting from the SSB of a global U(1) symmetry, introduced to solve the strong CP problem of QCD.

Axions behaving as
Warm Dark Matter

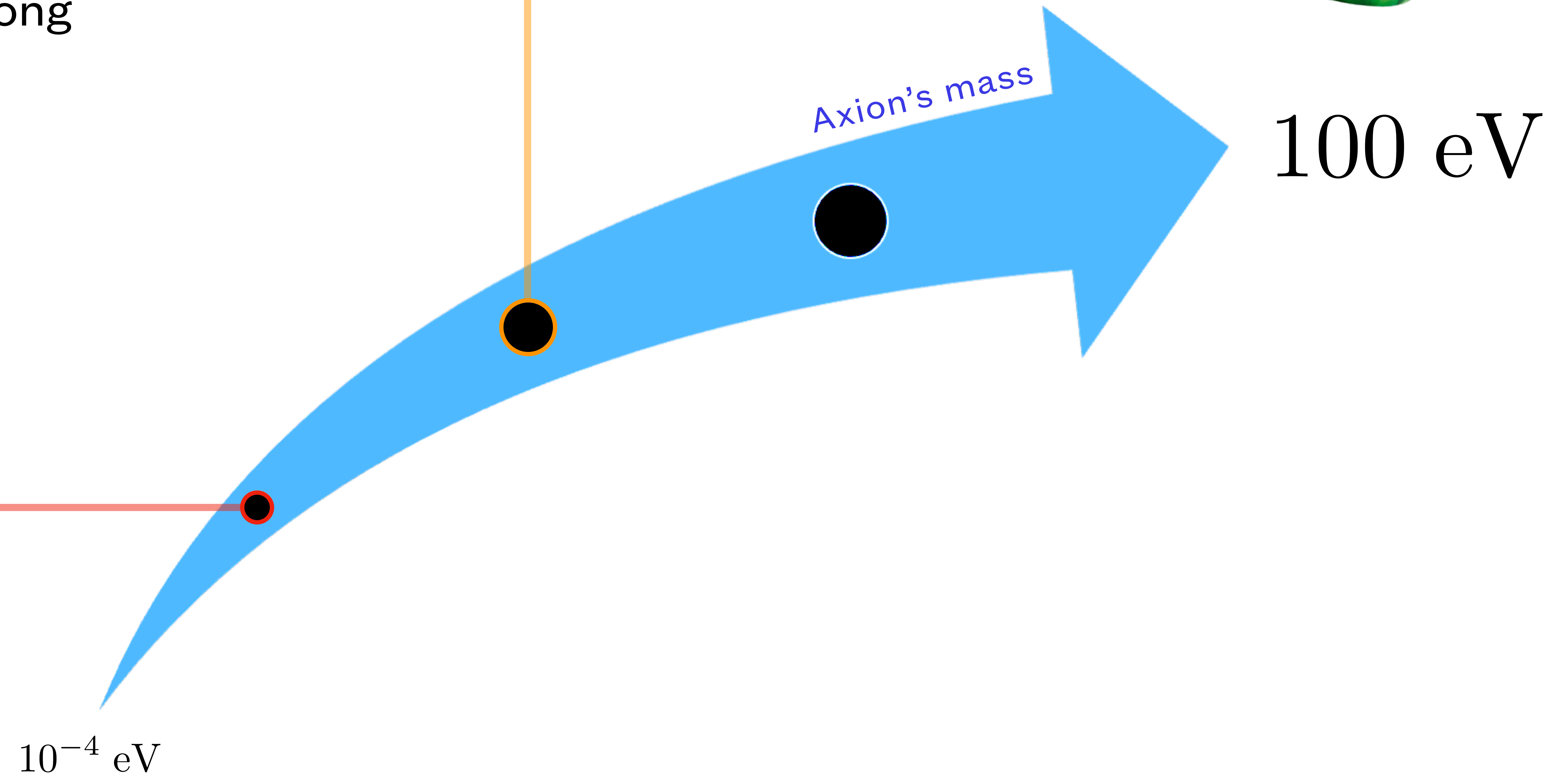

$$\Delta N_{\rm eff} \equiv \frac{\rho_a\,(m_a = 0)}{\rho_{\nu,\rm mless}} \propto \left(\frac{g_a}{g_\gamma}\right)\left(\frac{T_a}{T_\gamma}\right)^4$$

$$\simeq 0.027 \left(\frac{g_{*s}\,(T_d)}{106.75}\right)^{-4/3}$$

Light axions contribute to the energy density of radiation

Cosmo-phenomenology of thermal axions

- The QCD axion is a pseudo Nambu-Goldstone boson (PNG) resulting from the SSB of a global U(1) symmetry, introduced to solve the strong CP problem of QCD.

Axions behaving as
Warm Dark Matter

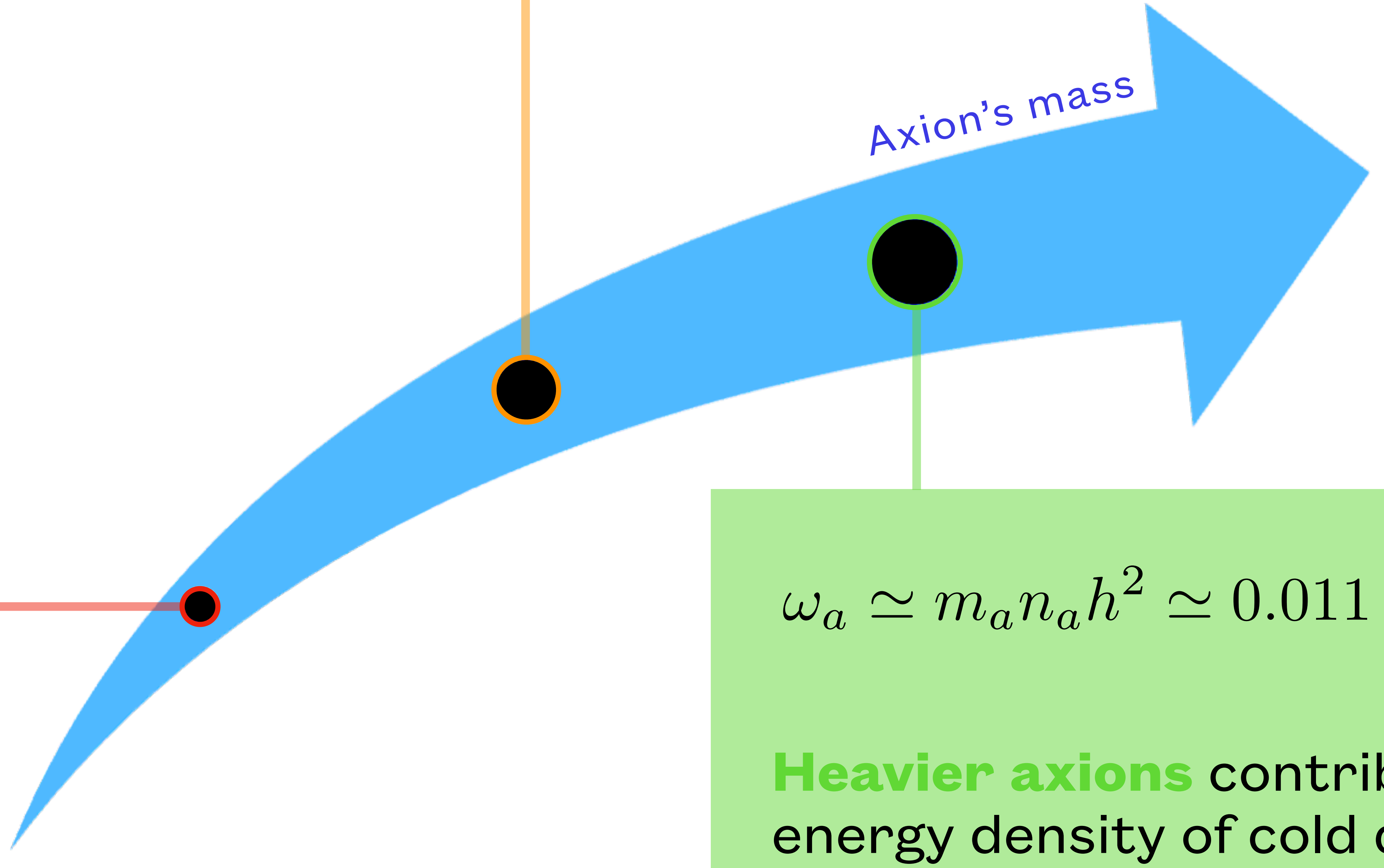

$$\Delta N_{\rm eff} \equiv \frac{\rho_a\,(m_a = 0)}{\rho_{\nu,\rm mless}} \propto \left(\frac{g_a}{g_\gamma}\right)\left(\frac{T_a}{T_\gamma}\right)^4$$

$$\simeq 0.027 \left(\frac{g_{*s}\,(T_d)}{106.75}\right)^{-4/3}$$

Light axions contribute to the energy density of radiation

$$\omega_a \simeq m_a n_a h^2 \simeq 0.011 \left(\frac{m_a}{\rm eV}\right) \Delta N_{\rm eff}^{3/4}$$

Heavier axions contribute to the energy density of cold dark matter (CDM)

Cosmo-phenomenology of thermal axions

- The QCD axion is a pseudo Nambu Goldstone boson (PNG) [...] SSB of a global U(1) symme[try ...] solve the strong CP pro[blem ...]

Not only QCD axions!

More in general, **axion-like particles** are PNGs with anomalous couplings to photon and gluons arising in many BSM extensions.

$$\Delta N_{\rm eff} \equiv \frac{\rho_a\,(m_a=0)}{\rho_{\nu,\rm mless}} \propto \left(\frac{g_a}{g_\gamma}\right)\left(\frac{T_a}{T_\gamma}\right)^4 \simeq 0.027\left(\frac{g_{*s}\,(T_d)}{106.75}\right)^{-4/3}$$

Light axions contribute to the energy density of radiation

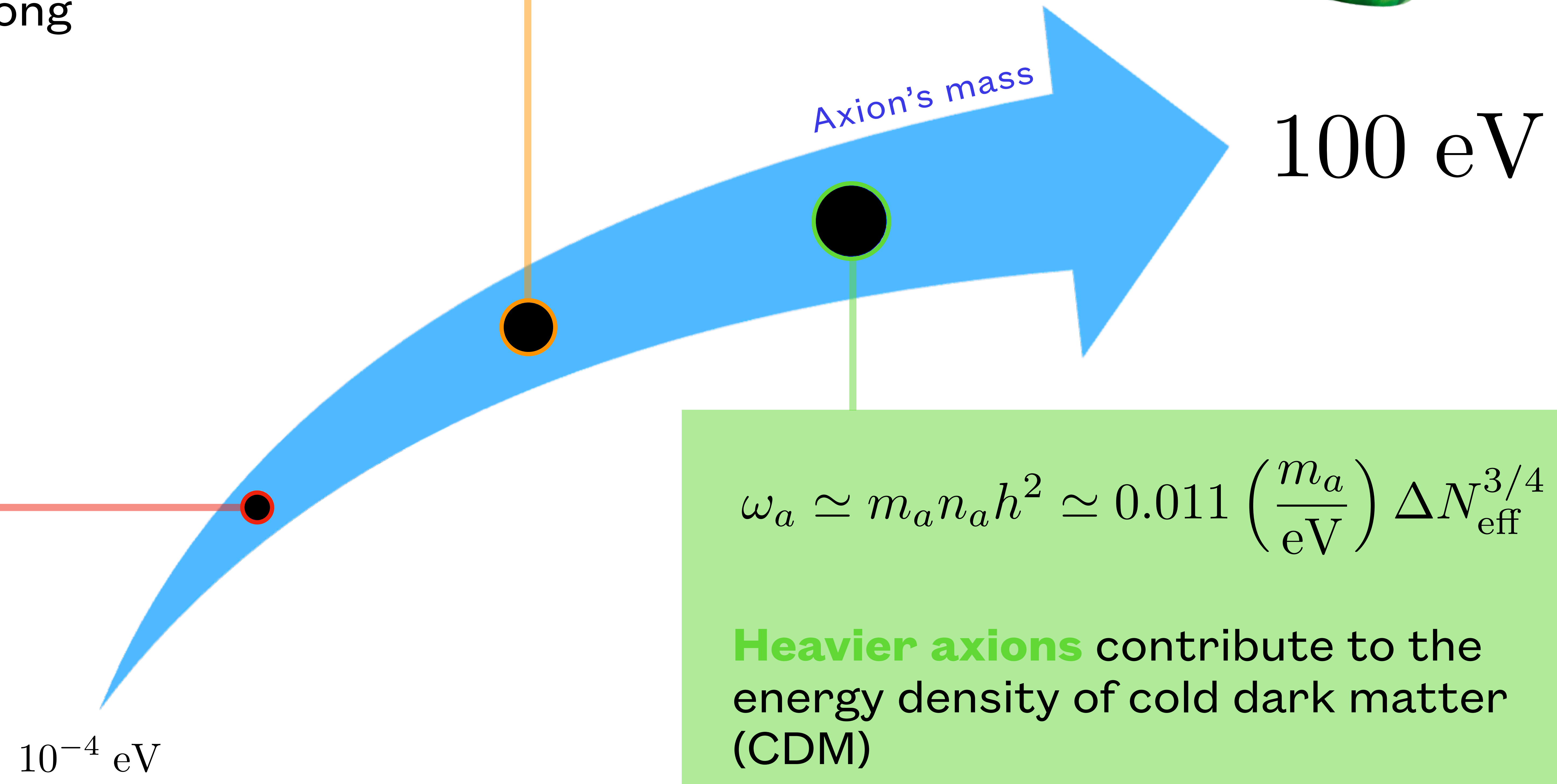

Axions behaving as **Warm Dark Matter**

$$\omega_a \simeq m_a n_a h^2 \simeq 0.011\left(\frac{m_a}{\rm eV}\right)\Delta N_{\rm eff}^{3/4}$$

Heavier axions contribute to the energy density of cold dark matter (CDM)

Motivation for this work

Motivation for this work

Update cosmological bounds on light **ALPs couplings**.

Motivation for this work

Update cosmological bounds on light **ALPs couplings**.

Quantify the impact of using the exact non-thermal PSD, in place of the standard **thermal approximation**.

Motivation for this work

Update cosmological bounds on light **ALPs couplings**.

Quantify the impact of using the exact non-thermal PSD, in place of the standard **thermal approximation**.

Test the potential of **future experiments** as complementary to laboratory searches.

Motivation for this work

Update cosmological bounds on light **ALPs couplings**.

Quantify the impact of using the exact non-thermal PSD, in place of the standard **thermal approximation**.

Test the potential of **future experiments** as complementary to laboratory searches.

Build a flexible toolset and pipeline suitable to be adapted to more general physical scenarios.

ALPs couplings

- Below the energy scale f_a at which the global symmetry is spontaneously broken, the ALP field is described by an effective field theory

$$\mathcal{L}_a \supset \frac{1}{2}(\partial^\mu a)(\partial_\mu a) - \frac{1}{2}m_a^2 a^2 + \sum_\ell c_\ell \frac{\partial_\mu a}{2f_a}\bar{\ell}\gamma^\mu\gamma^5\ell + \frac{1}{4}g_{a\gamma} a F_{\mu\nu}\tilde{F}^{\mu\nu}$$

ALPs couplings

- Below the energy scale f_a at which the global symmetry is spontaneously broken, the ALP field is described by an effective field theory

$$\mathcal{L}_a \supset \frac{1}{2}(\partial^\mu a)(\partial_\mu a) - \frac{1}{2}m_a^2 a^2 + \sum_\ell c_\ell \frac{\partial_\mu a}{2 f_a}\bar{\ell}\gamma^\mu\gamma^5\ell + \frac{1}{4}g_{a\gamma} a F_{\mu\nu}\tilde{F}^{\mu\nu}$$

Charged leptons coupling

Production takes place through lepton pairs annihilation and Compton-like scattering

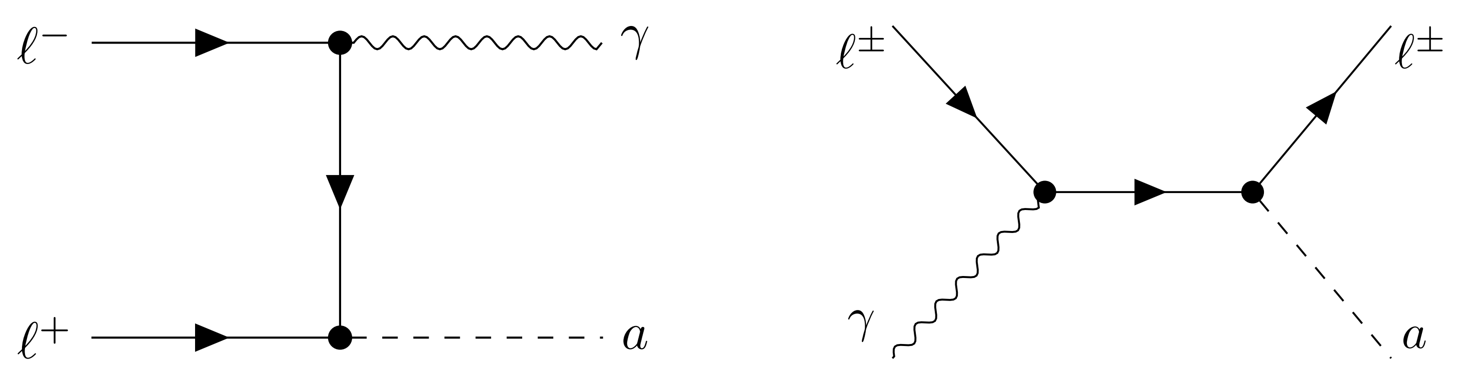

ALPs couplings

- Below the energy scale f_a at which the global symmetry is spontaneously broken, the ALP field is described by an effective field theory

$$\mathcal{L}_a \supset \frac{1}{2}(\partial^\mu a)(\partial_\mu a) - \frac{1}{2}m_a^2 a^2 + \sum_\ell c_\ell \frac{\partial_\mu a}{2 f_a}\bar{\ell}\gamma^\mu\gamma^5\ell + \frac{1}{4} g_{a\gamma} a F_{\mu\nu}\tilde{F}^{\mu\nu}$$

Charged leptons coupling

Production takes place through lepton pairs annihilation and Compton-like scattering

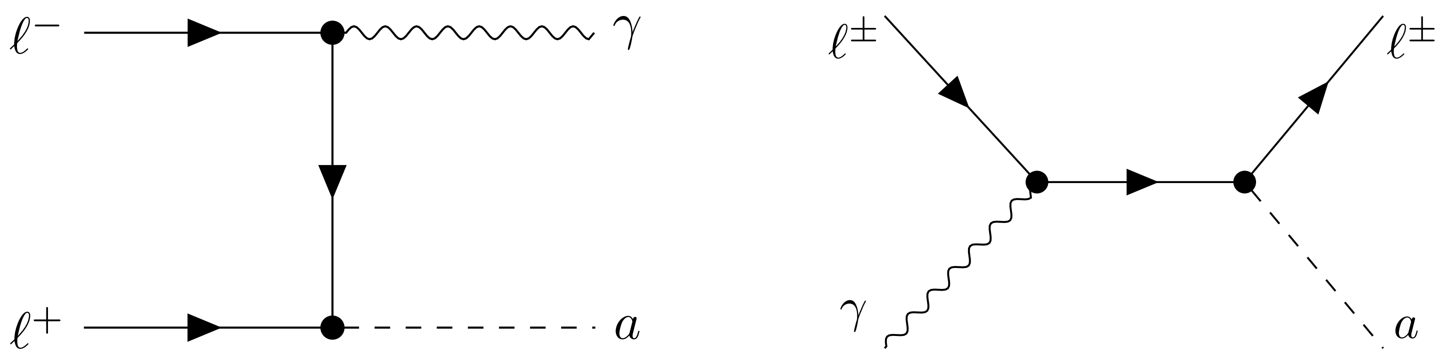

Photon coupling

Production takes place through the Primakoff process

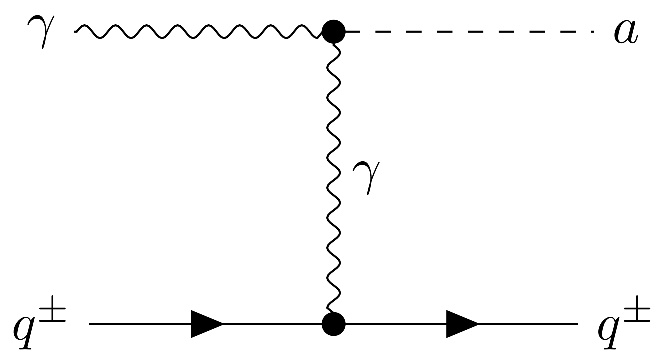

Thermal(?) ALPs production

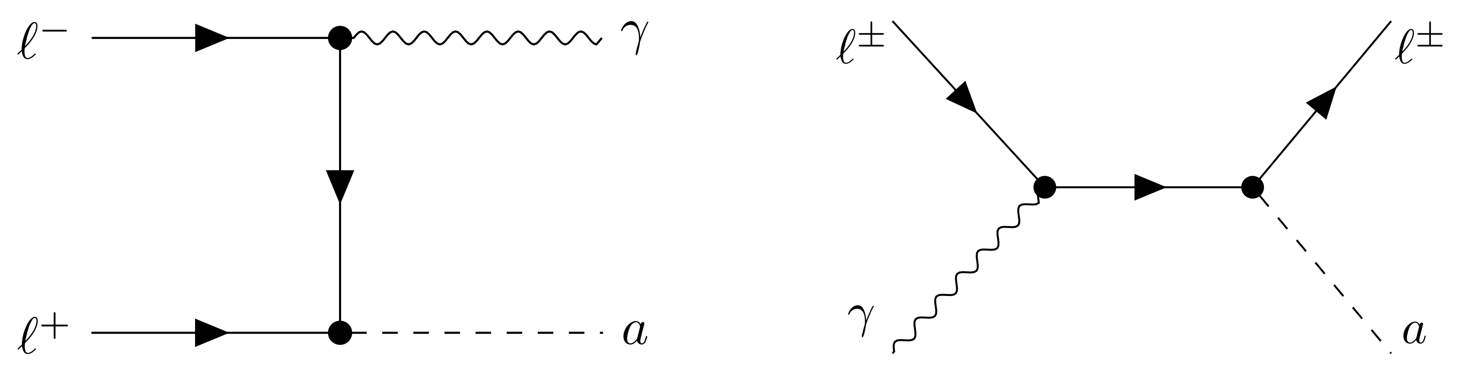

- The time evolution of ALP PSD is governed by the Boltzmann equation

$$\frac{d\mathcal{F}_a(k,t)}{dt} = \mathcal{C}_a(k,t)\left[1 - \frac{\mathcal{F}_a(k,t)}{\mathcal{F}_a^{\rm eq}(k,t)}\right]$$

- We solve the full BE in phase space without thermal approximations. This allows us to consistently compute the PSD across the freeze-in and freeze-out regimes.

Leptonic production: IR-dominated process, cross section peaked at the lepton mass

Primakoff production: UV-dominated process, cross section peaked at the initial temperature

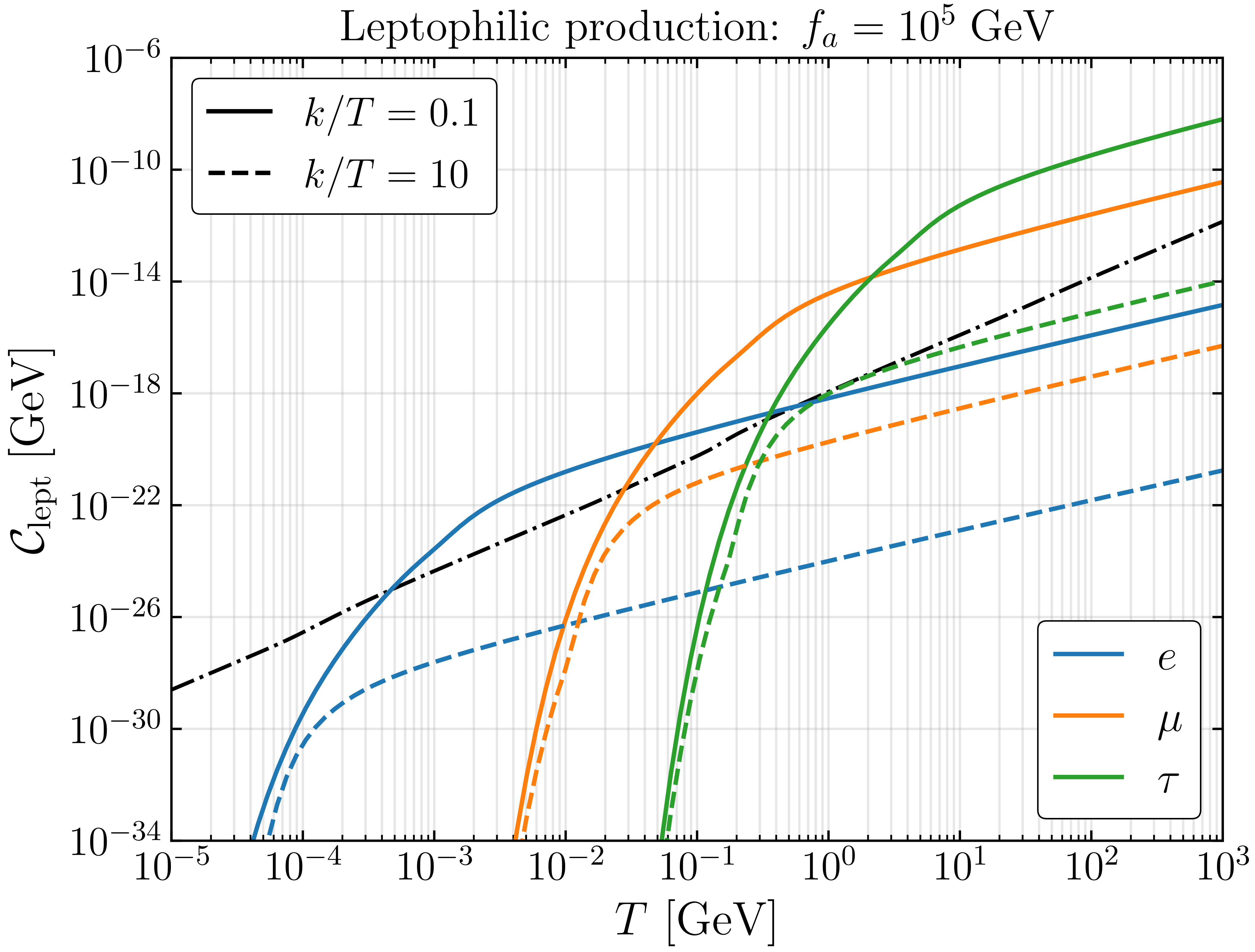

[See also: D'Eramo, Hajkarim, Lenoci: 2311.04974]

Thermal(?) ALPs production

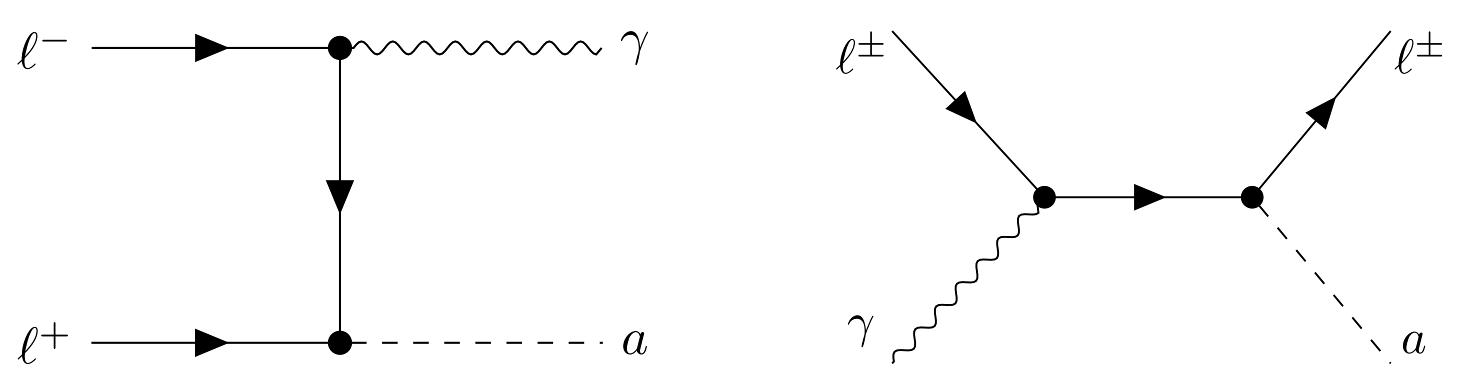

- The time evolution of ALP PSD is governed by the Boltzmann equation

$$\frac{d\mathcal{F}_a(k,t)}{dt} = \mathcal{C}_a(k,t)\left[1 - \frac{\mathcal{F}_a(k,t)}{\mathcal{F}_a^{\mathrm{eq}}(k,t)}\right]$$

- We solve the full BE in phase space without thermal approximations. This allows us to consistently compute the PSD across the freeze-in and freeze-out regimes.

Leptonic production: IR-dominated process, cross section peaked at the lepton mass

Primakoff production: UV-dominated process, cross section peaked at the initial temperature

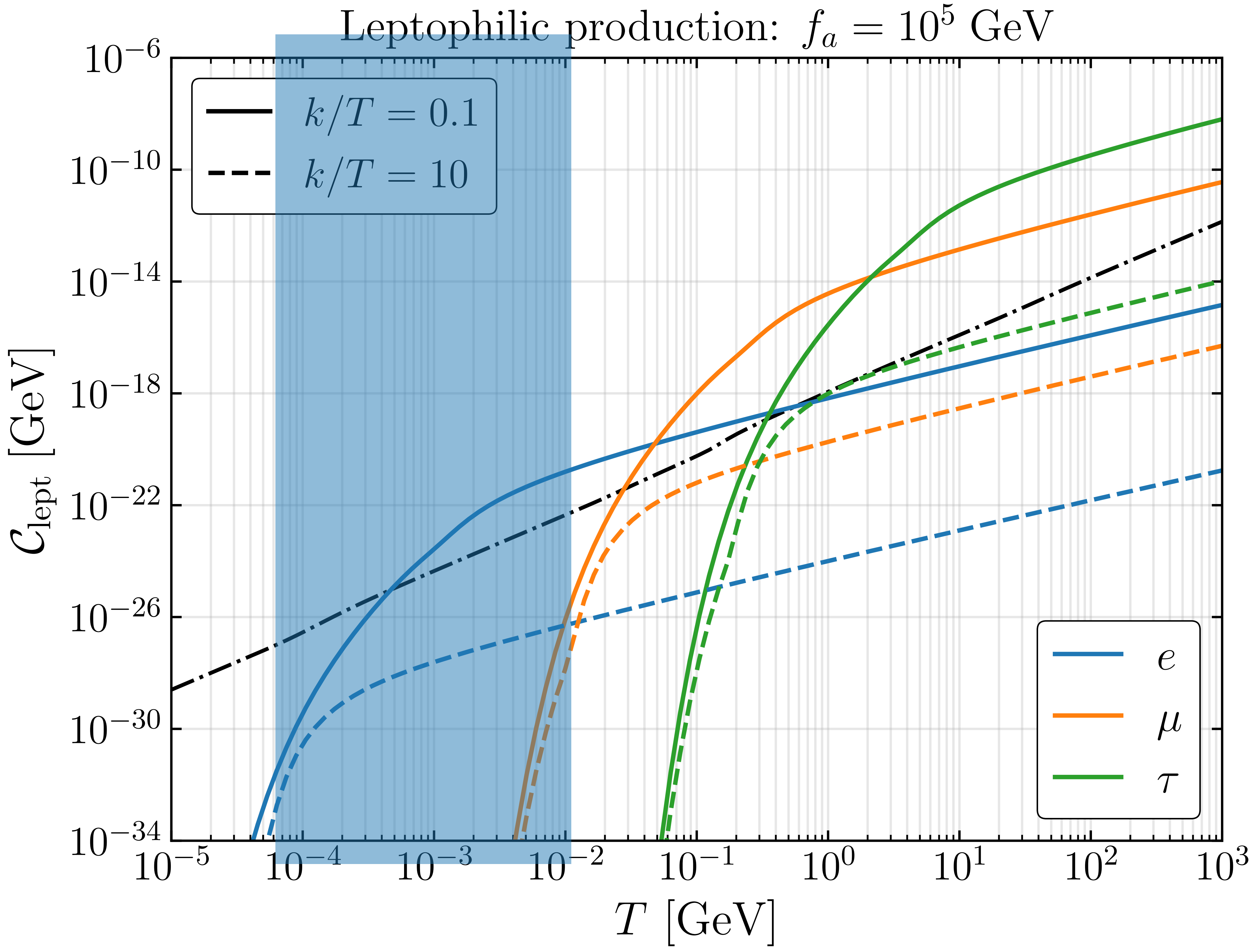

[See also: D'Eramo, Hajkarim, Lenoci: 2311.04974]

Thermal(?) ALPs production

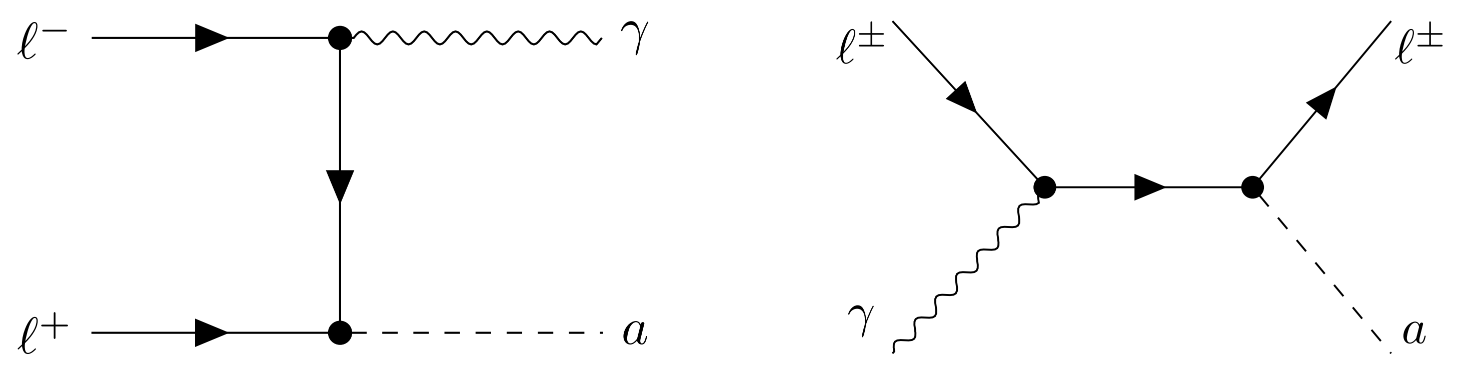

- The time evolution of ALP PSD is governed by the Boltzmann equation

$$\frac{d\mathcal{F}_a(k,t)}{dt} = \mathcal{C}_a(k,t)\left[1 - \frac{\mathcal{F}_a(k,t)}{\mathcal{F}_a^{\rm eq}(k,t)}\right]$$

- We solve the full BE in phase space without thermal approximations. This allows us to consistently compute the PSD across the freeze-in and freeze-out regimes.

Leptonic production: IR-dominated process, cross section peaked at the lepton mass

Primakoff production: UV-dominated process, cross section peaked at the initial temperature

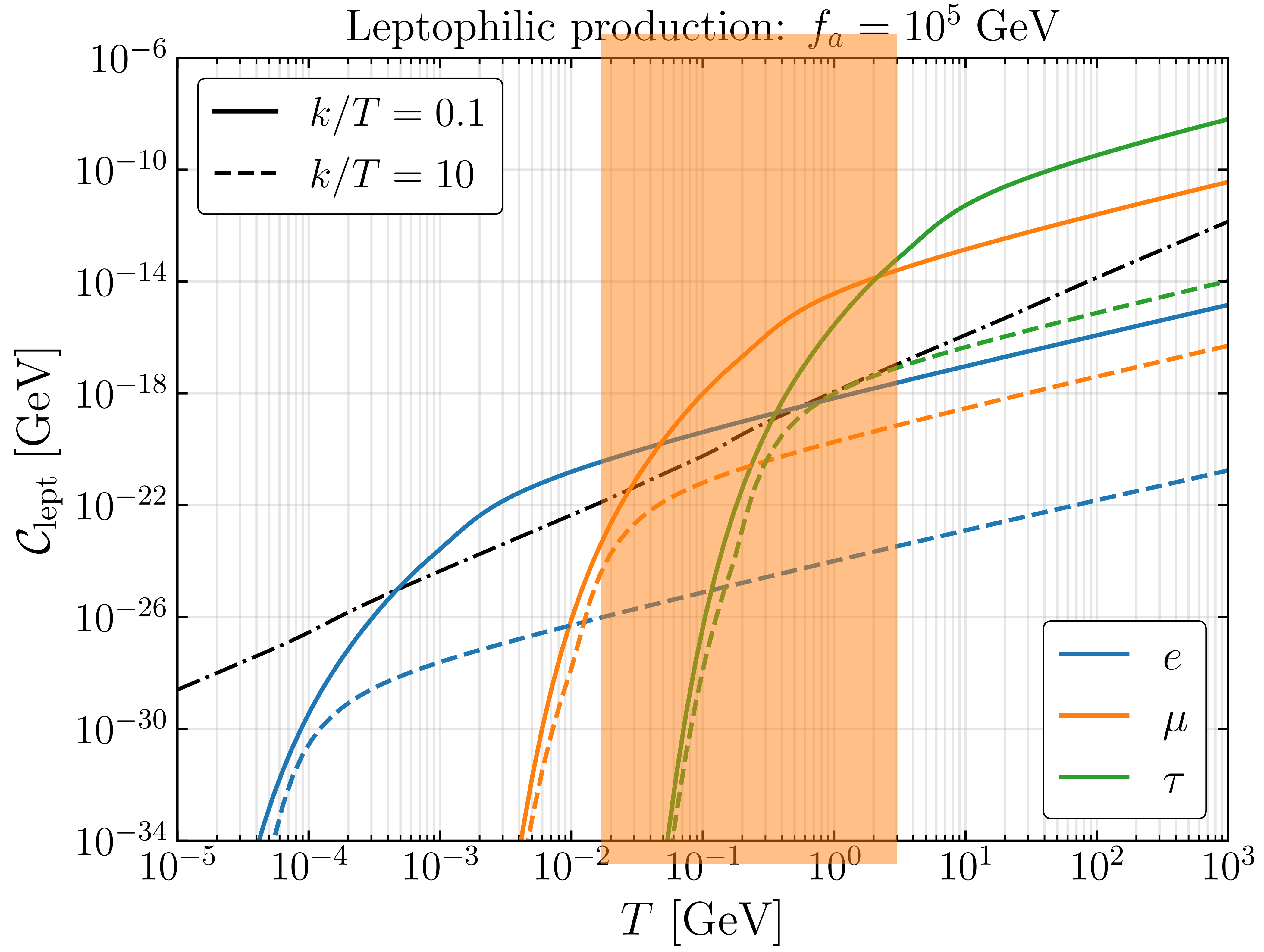

[See also: D'Eramo, Hajkarim, Lenoci: 2311.04974]

Thermal(?) ALPs production

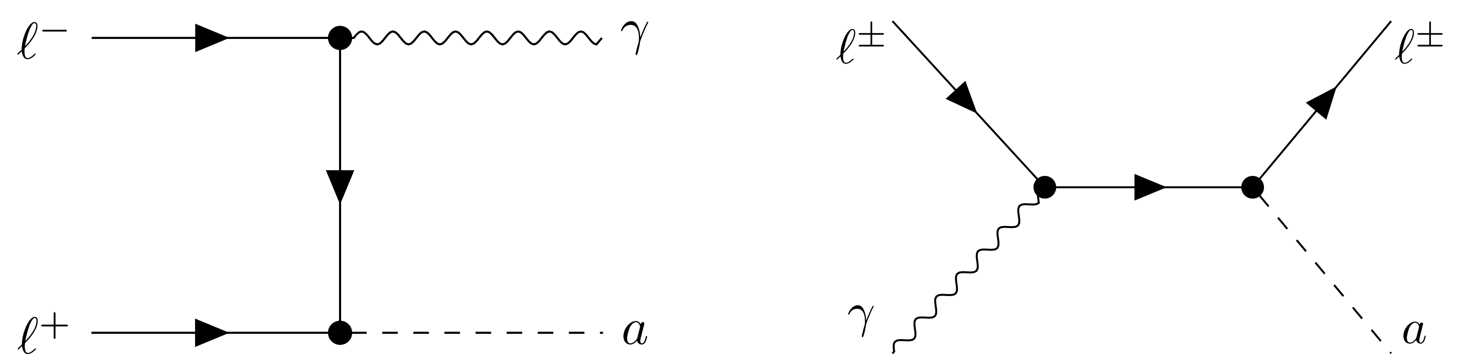

- The time evolution of ALP PSD is governed by the Boltzmann equation

$$\frac{d\mathcal{F}_a(k,t)}{dt} = \mathcal{C}_a(k,t)\left[1 - \frac{\mathcal{F}_a(k,t)}{\mathcal{F}_a^{\rm eq}(k,t)}\right]$$

- We solve the full BE in phase space without thermal approximations. This allows us to consistently compute the PSD across the freeze-in and freeze-out regimes.

Leptonic production: IR-dominated process, cross section peaked at the lepton mass

Primakoff production: UV-dominated process, cross section peaked at the initial temperature

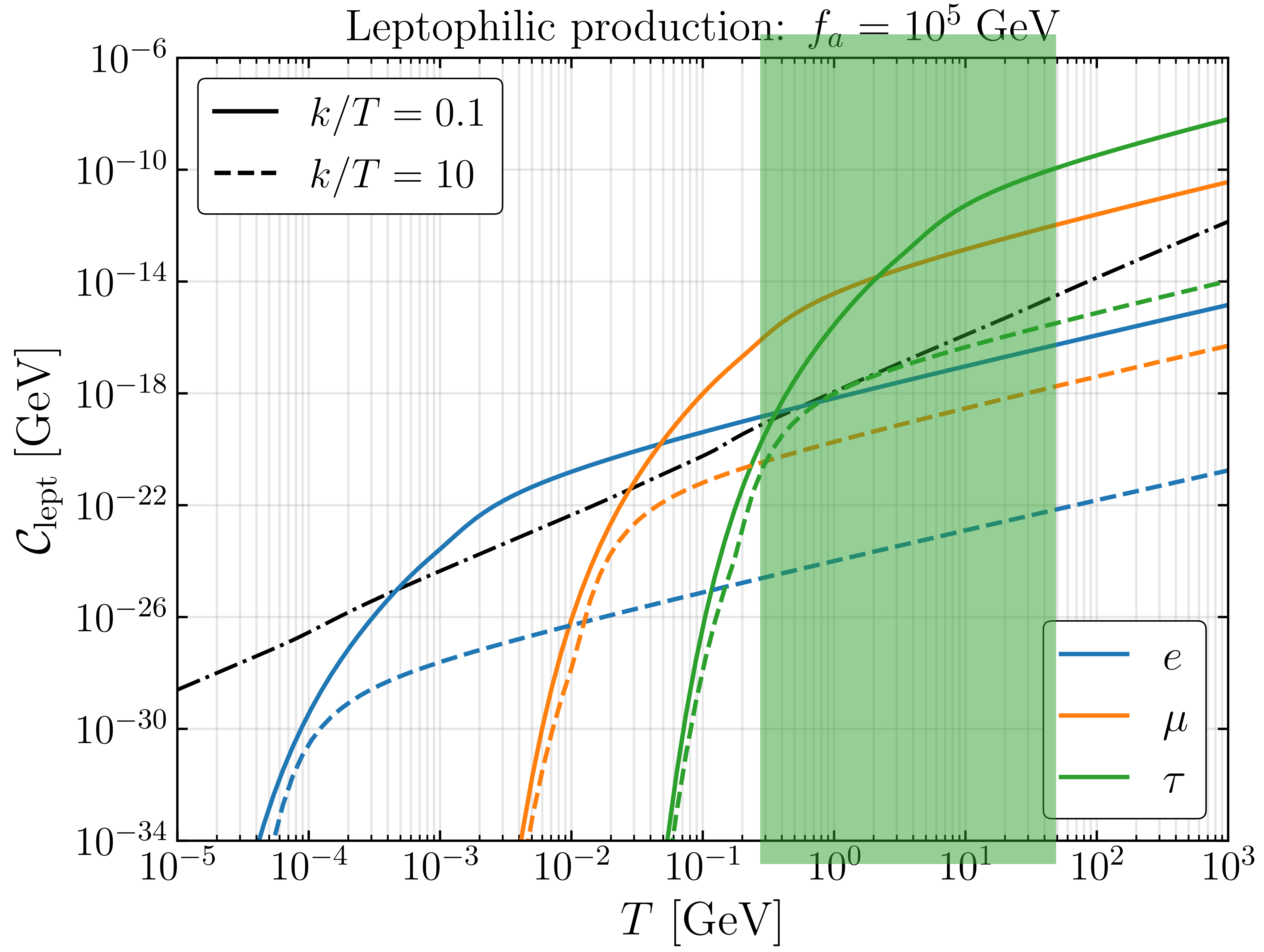

[See also: D'Eramo, Hajkarim, Lenoci: 2311.04974]

Thermal(?) ALPs production

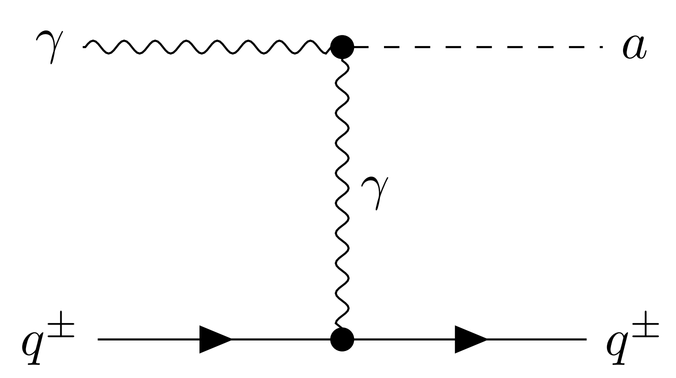

- The time evolution of ALP PSD is governed by the Boltzmann equation

$$\frac{d\mathcal{F}_a(k,t)}{dt} = \mathcal{C}_a(k,t)\left[1 - \frac{\mathcal{F}_a(k,t)}{\mathcal{F}_a^{\rm eq}(k,t)}\right]$$

- We solve the full BE in phase space without thermal approximations. This allows us to consistently compute the PSD across the freeze-in and freeze-out regimes.

Leptonic production: IR-dominated process, cross section peaked at the lepton mass

Primakoff production: UV-dominated process, cross section peaked at the initial temperature

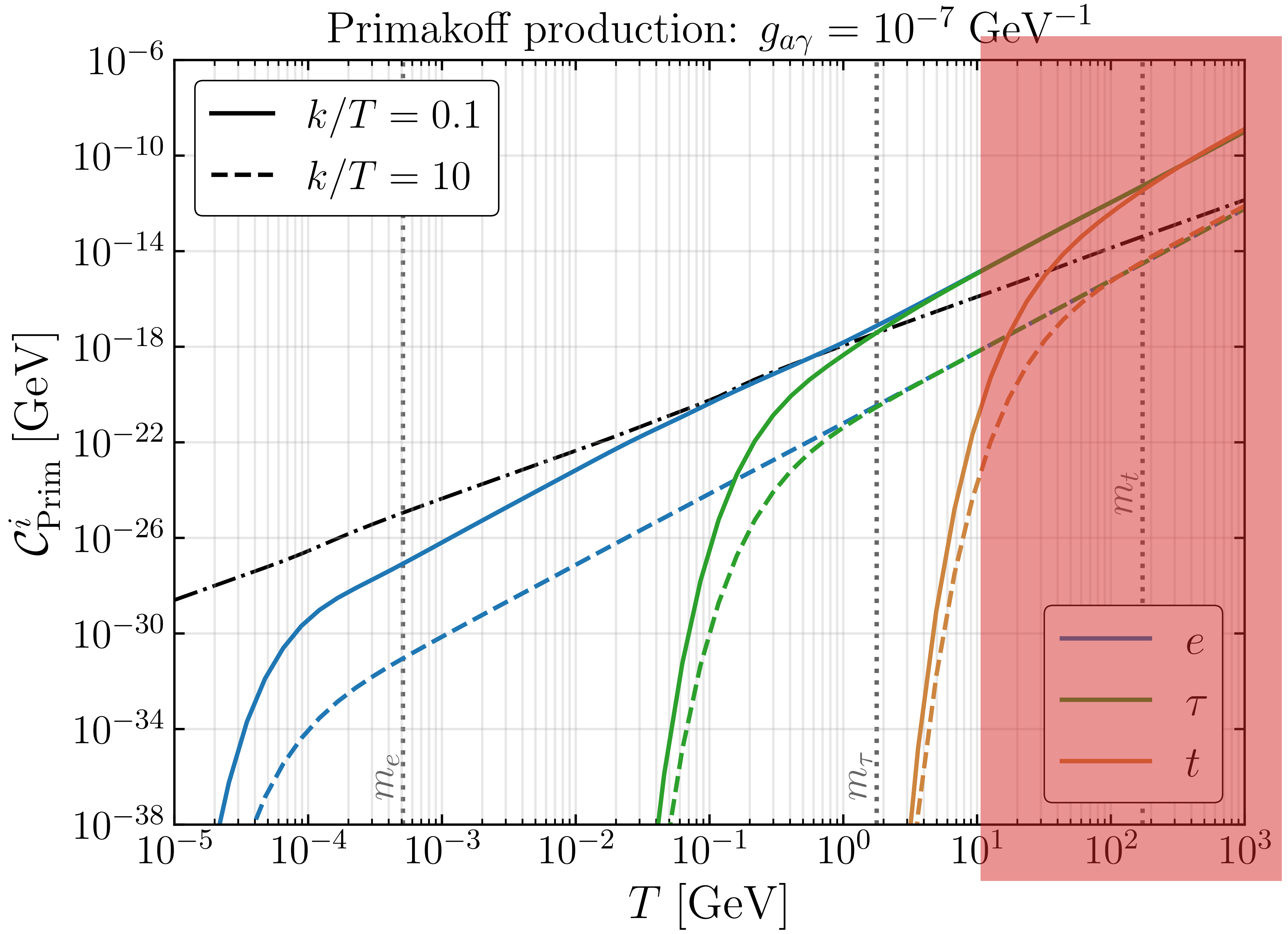

[See also: Jain, Maggi, Ai, Marsh: 2406.01678]

Phase-space distributions

- To quantify the deviation from a thermal spectrum, we define the quantity

$$\delta_{\rm th} \equiv \frac{q^3\,[\mathcal{F}_a(q,x_f) - \mathcal{F}_a^{\rm eq}(q,\bar{x})]}{\int dq\, q^3 \mathcal{F}_a^{\rm eq}(q,\bar{x})}$$

- Comparison with a thermal (Bose-Einstein) distribution with temperature properly rescaled to match $\Delta N_{\rm eff}$.

- Larger deviations arise for smaller couplings because of a less efficient thermalisation (**freeze-in** regime)

[See also: D'Eramo, Hajkarim, Lenoci: 2311.04974 and Badziak, Laletin: 2410.18186]

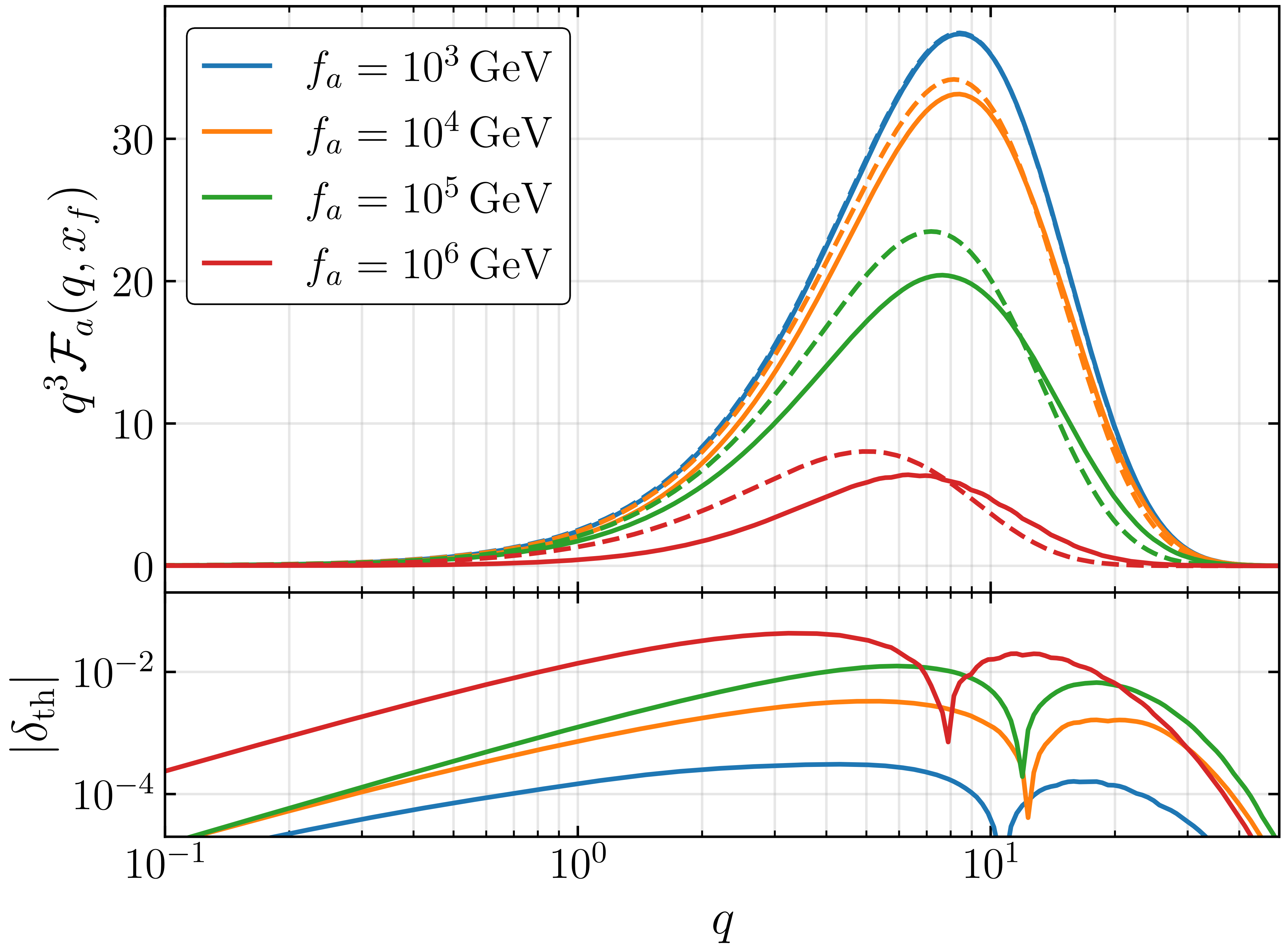

Thermal(?) ALPs production

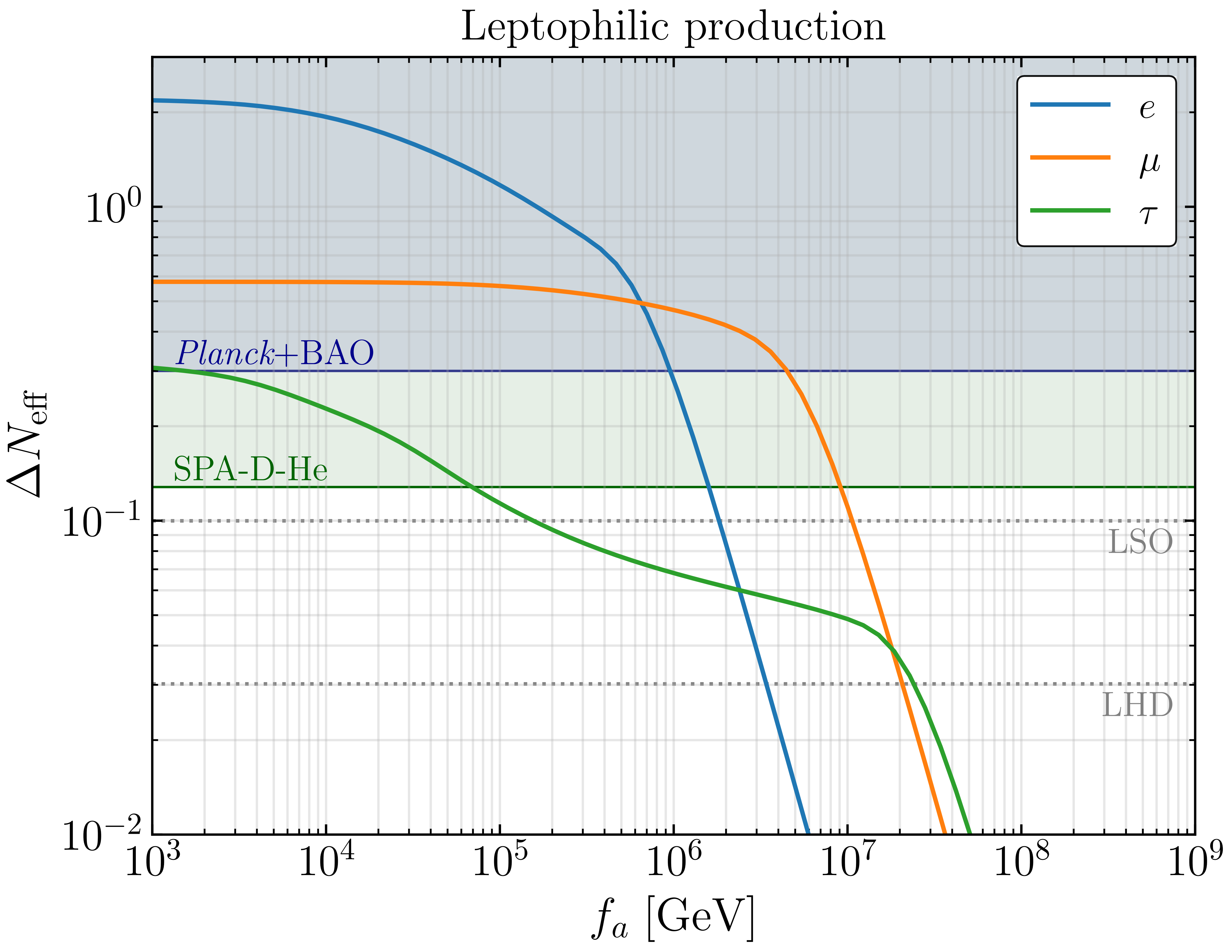

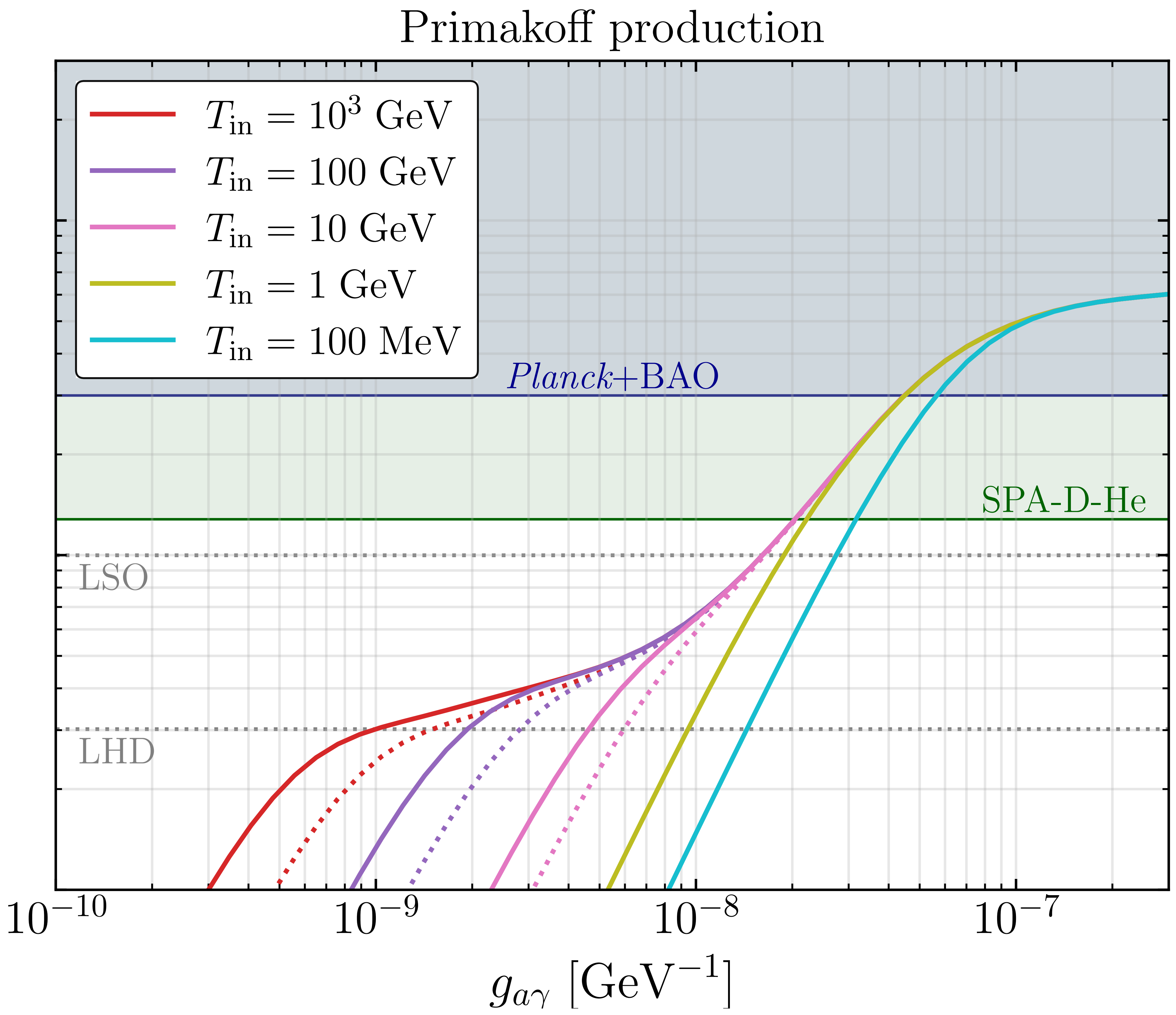

Pipeline and datasets

Amplitudes from effective modelling of ALPs interactions

$|\mathcal{M}|^2$

ALPs PSD from full phase spaces solution of Boltzmann equation

$\mathcal{F}_a(q, T_{\rm fin})$

Interface to CLASS to evolve the cosmological model

$C_\ell,\ P(k)$

MCMC analysis through Cobaya sampler to get constraints

$\Delta f_a < [...]$

Datasets combinations

- Planck2018: low-ℓ TT (`Commander`) + low-ℓ EE (`SRoll2`) + high-ℓ TTTEEE (`Plik_lite`)
- ACT-DR6: TTTEEE from `act_dr6_cmbonly`
- SPT-3G D1: TTTEEE from `candl_like`
- Lensing: baseline combination of Planck+ACT (`act_dr6_lenslike`) and muse SPT-3G 2yr
- Measurements of BAO distance from DESI DR2
- D/H ratio and He mass fraction values from weighted averages of PDG 2025.

Extra: realistic forecasts for near and far future CMB experiments (Simons Observatory, Litebird and CMB-HD).

Pipeline and datasets

Amplitudes from effective modelling of ALPs interactions $|\mathcal{M}|^2$	ALPs PSD from full phase spaces solution of Boltzmann equation $\mathcal{F}_a(q, T_{\rm fin})$	Interface to CLASS to evolve the cosmological model $C_\ell,\ P(k)$	MCMC analysis through Cobaya sampler to get constraints $\Delta f_a < [...]$

Datasets combinations

SPA

- Planck2018: low-ℓ TT (`Commander`) + low-ℓ EE (`SRoll2`) + high-ℓ TTTEEE (`Plik_lite`)
- ACT-DR6: TTTEEE from `act_dr6_cmbonly`
- SPT-3G D1: TTTEEE from `candl_like`
- Lensing: baseline combination of Planck+ACT (`act_dr6_lenslike`) and muse SPT-3G 2yr

- Measurements of BAO distance from DESI DR2
- D/H ratio and He mass fraction values from weighted averages of PDG 2025.

Extra: realistic forecasts for near and far future CMB experiments (Simons Observatory, Litebird and CMB-HD).

Pipeline and datasets

Amplitudes from effective modelling of ALPs interactions	ALPs PSD from full phase spaces solution of Boltzmann equation	Interface to CLASS to evolve the cosmological model	MCMC analysis through Cobaya sampler to get constraints
$\lvert\mathcal{M}\rvert^2$	$\mathcal{F}_a(q, T_{\rm fin})$	$C_\ell,\ P(k)$	$\Delta f_a < [...]$

Datasets combinations

SPA

- Planck2018: low-ℓ TT (`Commander`) + low-ℓ EE (`SRoll2`) + high-ℓ TTTEEE (`Plik_lite`)
- ACT-DR6: TTTEEE from `act_dr6_cmbonly`
- SPT-3G D1: TTTEEE from `candl_like`
- Lensing: baseline combination of Planck+ACT (`act_dr6_lenslike`) and muse SPT-3G 2yr

-B

- Measurements of BAO distance from DESI DR2
- D/H ratio and He mass fraction values from weighted averages of PDG 2025.

Extra: realistic forecasts for near and far future CMB experiments (Simons Observatory, Litebird and CMB-HD).

Pipeline and datasets

Amplitudes from effective modelling of ALPs interactions

$|\mathcal{M}|^2$

ALPs PSD from full phase spaces solution of Boltzmann equation

$\mathcal{F}_a(q, T_{\rm fin})$

Interface to CLASS to evolve the cosmological model

$C_\ell,\ P(k)$

MCMC analysis through Cobaya sampler to get constraints

$\Delta f_a < [...]$

Datasets combinations

SPA

- Planck2018: low-ℓ TT (`Commander`) + low-ℓ EE (`SRoll2`) + high-ℓ TTTEEE (`Plik_lite`)
- ACT-DR6: TTTEEE from `act_dr6_cmbonly`
- SPT-3G D1: TTTEEE from `candl_like`
- Lensing: baseline combination of Planck+ACT (`act_dr6_lenslike`) and muse SPT-3G 2yr

-B

- Measurements of BAO distance from DESI DR2
- D/H ratio and He mass fraction values from weighted averages of PDG 2025.

-D-He

Extra: realistic forecasts for near and far future CMB experiments (Simons Observatory, Litebird and CMB-HD).

Constraints and future implications

- 95% Bayesian credible limits on ALPs couplings

Model		SPA	SPA-D-He	SPA-D-He-B	LSO	LHD
$\Lambda\text{CDM} + e$	f_a [GeV]	$> 1.51 \times 10^6$	$> 1.63 \times 10^6$	$> 1.37 \times 10^6$	$> 1.90 \times 10^6$	3.56×10^6
$\Lambda\text{CDM} + \mu$	f_a [GeV]	$> 8.73 \times 10^6$	$> 9.41 \times 10^6$	$> 7.50 \times 10^6$	$> 1.05 \times 10^7$	2.17×10^7
$\Lambda\text{CDM} + \tau$	f_a [GeV]	$> 6.10 \times 10^4$	$> 8.06 \times 10^4$	$> 2.85 \times 10^4$	$> 1.34 \times 10^5$	2.45×10^7
$\Lambda\text{CDM} + \gamma$	$g_{a\gamma}$ [GeV^{-1}]	$< 2.18 \times 10^{-8}$	$< 1.98 \times 10^{-8}$	$< 2.73 \times 10^{-8}$	$< 1.66 \times 10^{-8}$	$< 1.01 \times 10^{-9}$

Constraints and future implications

- 95% Bayesian credible limits on ALPs couplings

Model		SPA	SPA-D-He	SPA-D-He-B	LSO	LHD
$\Lambda\mathrm{CDM} + e$	f_a [GeV]	$> 1.51 \times 10^6$	$> 1.63 \times 10^6$	$> 1.37 \times 10^6$	$> 1.90 \times 10^6$	3.56×10^6
			$> 9.41 \times 10^6$	$> 7.50 \times 10^6$	$> 1.05 \times 10^7$	2.17×10^7
			$> 8.06 \times 10^4$	$> 2.85 \times 10^4$	$> 1.34 \times 10^5$	2.45×10^7
			$< 1.98 \times 10^{-8}$	$< 2.73 \times 10^{-8}$	$< 1.66 \times 10^{-8}$	$< 1.01 \times 10^{-9}$

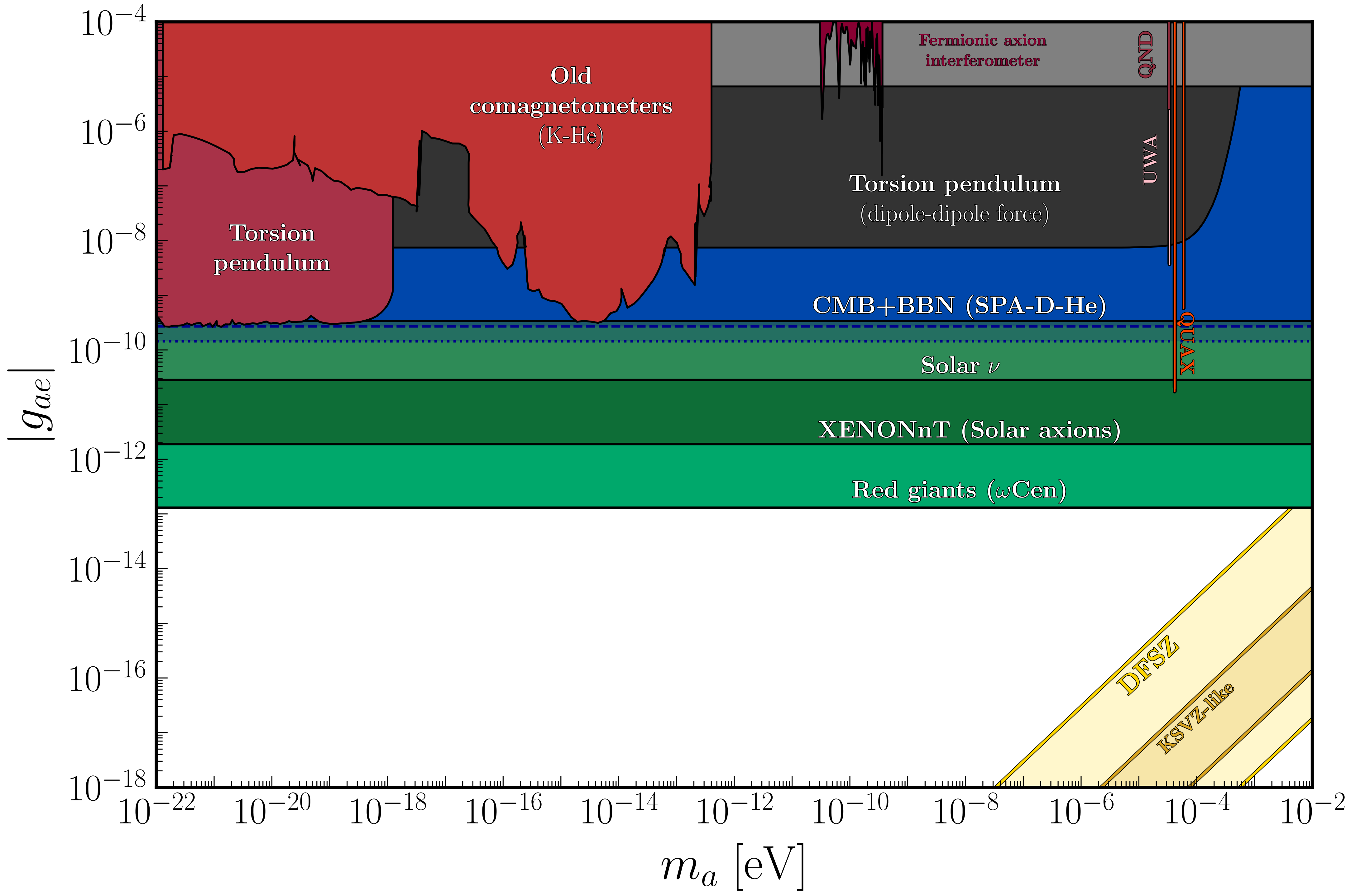

Constraints and future implications

- 95% Bayesian credible limits on ALPs couplings

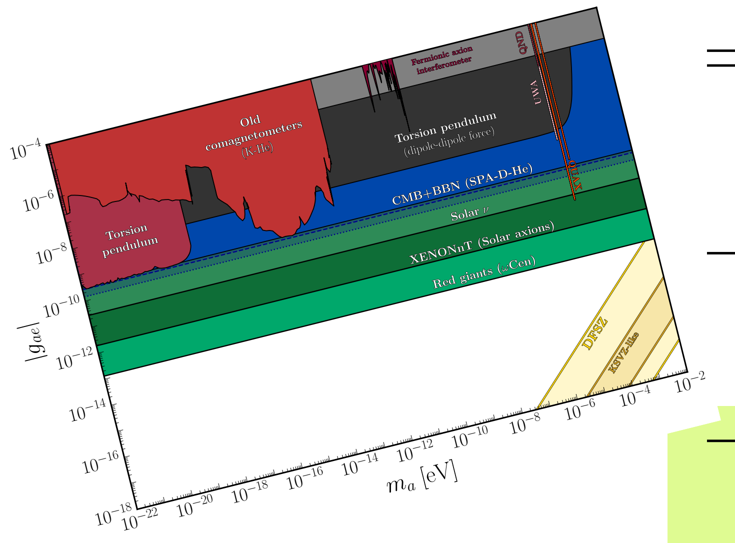

Model		**SPA**	**SPA-D-He**	**SPA-D-He-B**	**LSO**	**LHD**
$\Lambda\text{CDM} + e$	f_a [GeV]	$> 1.51 \times 10^6$	$> 1.63 \times 10^6$	$> 1.37 \times 10^6$	$> 1.90 \times 10^6$	3.56×10^6
$\Lambda\text{CDM} + \mu$	f_a [GeV]	$> 8.73 \times 10^6$	$> 9.41 \times 10^6$	$> 7.50 \times 10^6$	$> 1.05 \times 10^7$	2.17×10^7
$\Lambda\text{CDM} + \tau$	f_a [GeV]	$> 6.10 \times 10^4$	$> 8.06 \times 10^4$	$> 2.85 \times 10^4$		
$\Lambda\text{CDM} + \gamma$	$g_{a\gamma}$ [GeV^{-1}]	$< 2.18 \times 10^{-8}$	$< 1.98 \times 10^{-8}$	$< 2.73 \times 10^{-8}$		

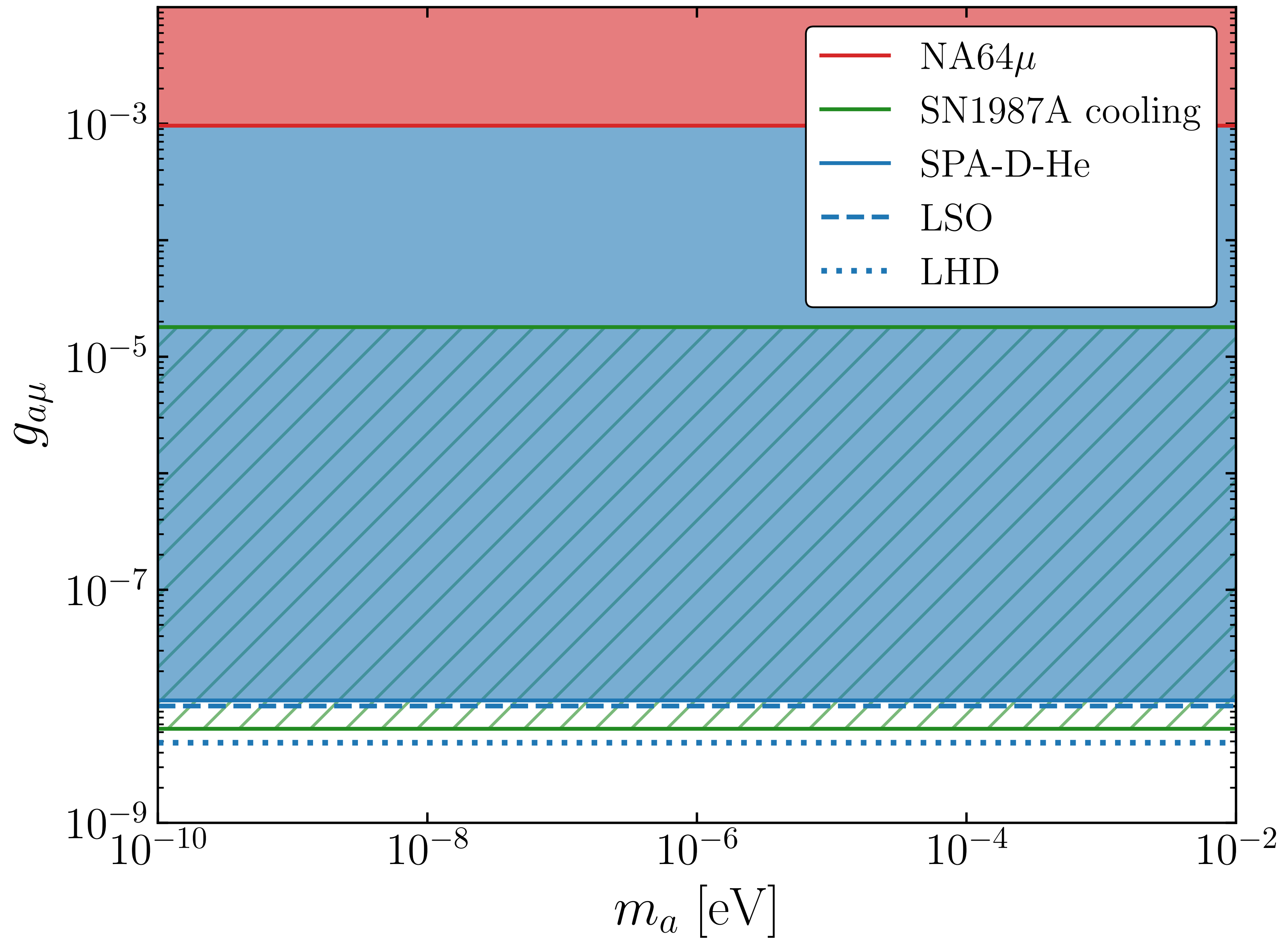

C… …ture implications

- 95… …gs

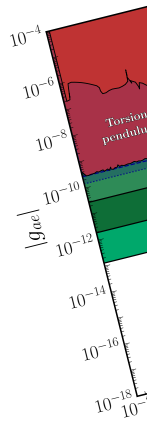

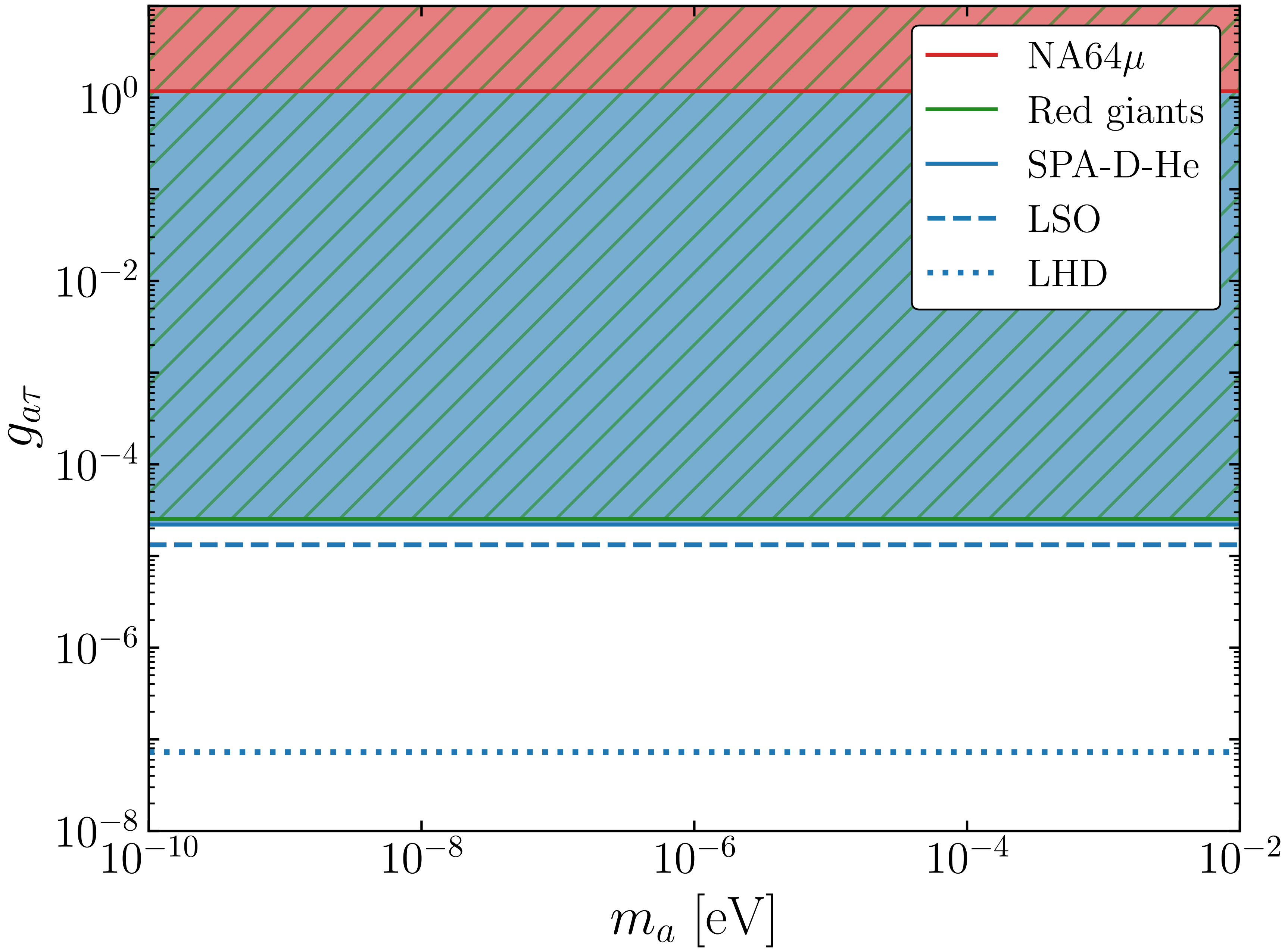

			SPA-D-He	SPA-D-He-B	LSO	LHD
		…^{6}	$> 1.63 \times 10^{6}$	$> 1.37 \times 10^{6}$	$> 1.90 \times 10^{6}$	3.56×10^{6}
		…^{6}	$> 9.41 \times 10^{6}$	$> 7.50 \times 10^{6}$	$> 1.05 \times 10^{7}$	2.17×10^{7}
$\Lambda\mathrm{CDM} + \tau$	f_a [GeV]	$> 6.10 \times 10^{4}$	$> 8.06 \times 10^{4}$	$> 2.85 \times 10^{4}$	$> 1.34 \times 10^{5}$	2.45×10^{7}
$\Lambda\mathrm{CDM} + \gamma$	$g_{a\gamma}$ [GeV^{-1}]	$< 2.18 \times 10^{-8}$	$< 1.98 \times 10^{-8}$	$< 2.73 \times 10^{-8}$	$< 1.66 \times 10^{-8}$	$< 1.01 \times 10^{-9}$

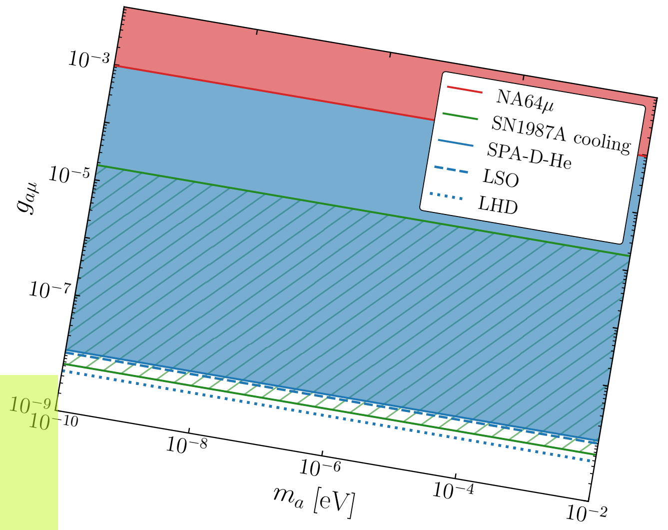

Constraints and future in

- 95% Bayesian credible limits on ALPs couplings

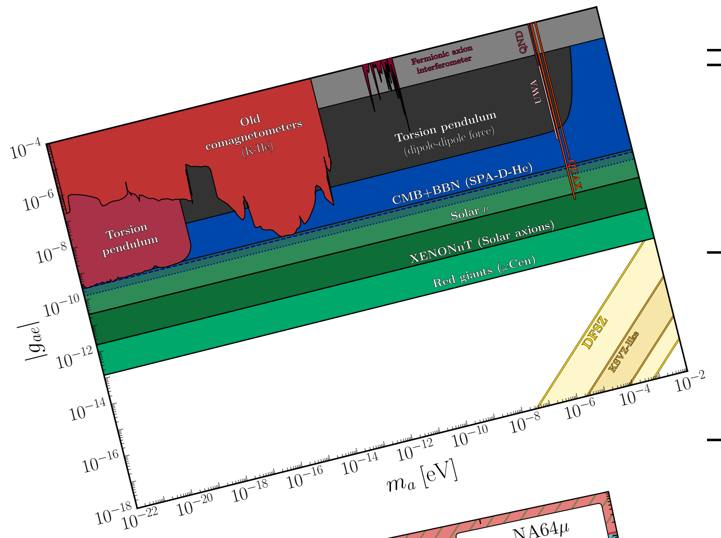

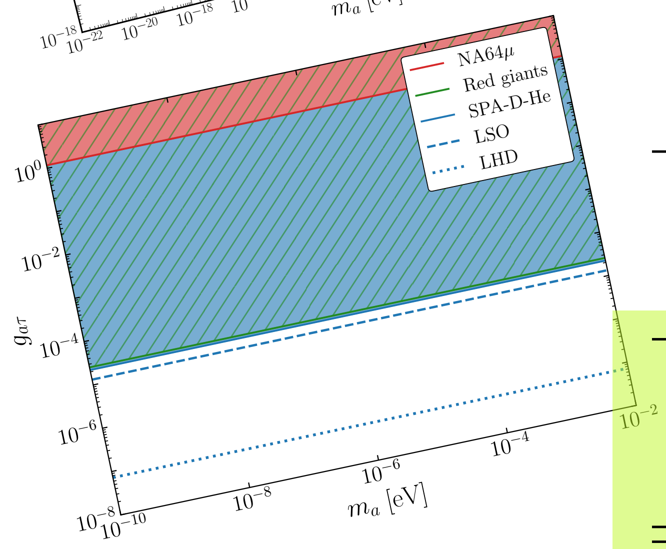

Model		SPA	SPA-D-He	SP		
$\Lambda\text{CDM}+e$	f_a [GeV]	$> 1.51 \times 10^6$	$> 1.63 \times 10^6$	$>$		
$\Lambda\text{CDM}+\mu$	f_a [GeV]	$> 8.73 \times 10^6$	$> 9.41 \times 10^6$	$>$		
$\Lambda\text{CDM}+\tau$	f_a [GeV]	$> 6.10 \times 10^4$	$> 8.06 \times 10^4$	$>$		
$\Lambda\text{CDM}+\gamma$	$g_{a\gamma}$ [GeV^{-1}]	$< 2.18 \times 10^{-8}$	$< 1.98 \times 10^{-8}$	$< 2.73 \times 10^{-8}$	$< 1.66 \times 10^{-8}$	$< 1.01 \times 10^{-9}$

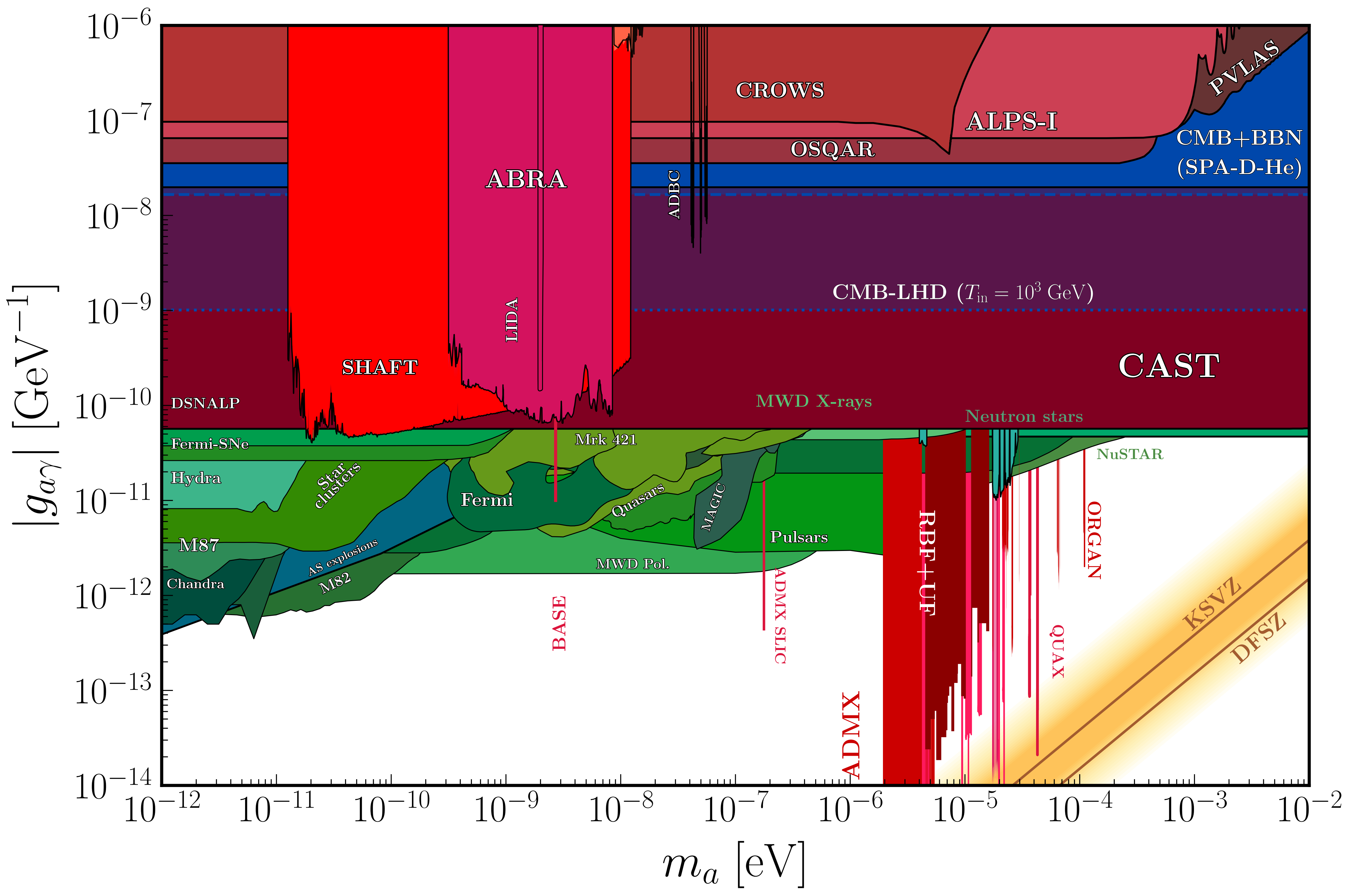

Constraints and future implications

- 95% Bayesian credible limits on ALPs couplings

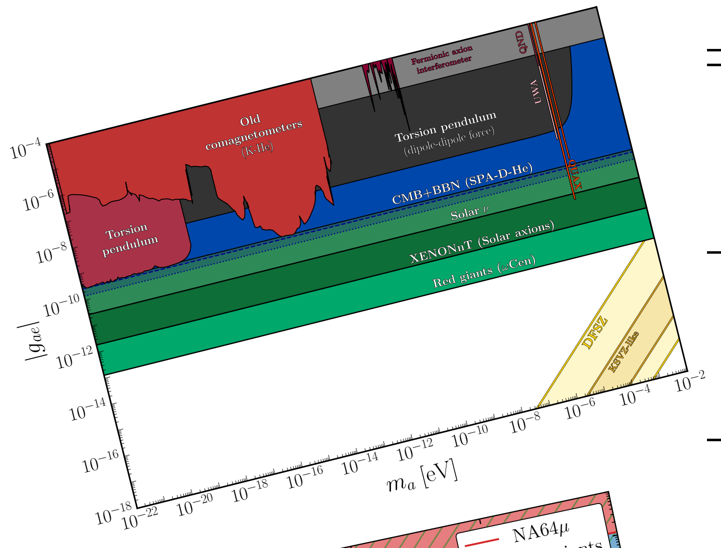

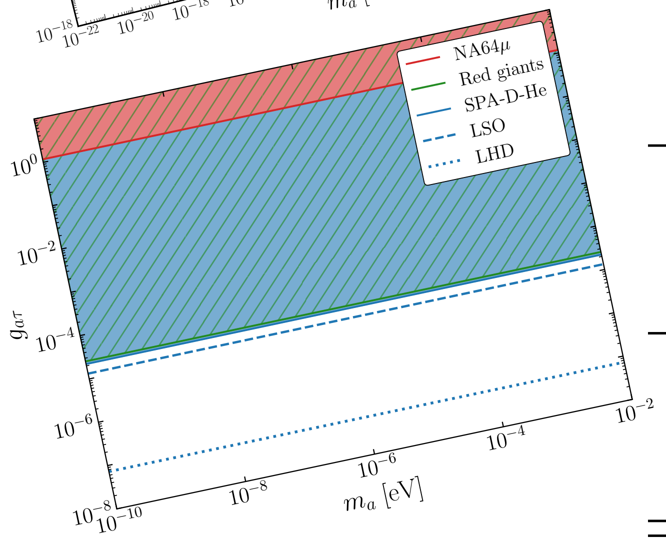

Model		SPA	SPA-D-He	SPA-D-He-B	LSO	LHD
$\Lambda\mathrm{CDM} + e$	f_a [GeV]	$> 1.51 \times 10^6$	$> 1.63 \times 10^6$	$> 1.37 \times 10^6$	$> 1.90 \times 10^6$	3.56×10^6
$\Lambda\mathrm{CDM} + \mu$	f_a [GeV]	$> 8.73 \times 10^6$	$> 9.41 \times 10^6$	$> 7.50 \times 10^6$	$> 1.05 \times 10^7$	2.17×10^7
$\Lambda\mathrm{CDM} + \tau$	f_a [GeV]	$> 6.10 \times 10^4$	$> 8.06 \times 10^4$	$> 2.85 \times 10^4$	$> 1.34 \times 10^5$	2.45×10^7
$\Lambda\mathrm{CDM} + \gamma$	$g_{a\gamma}$ [GeV^{-1}]	$< 2.18 \times 10^{-8}$	$< 1.98 \times 10^{-8}$	$< 2.73 \times 10^{-8}$	$< 1.66 \times 10^{-8}$	$< 1.01 \times 10^{-9}$

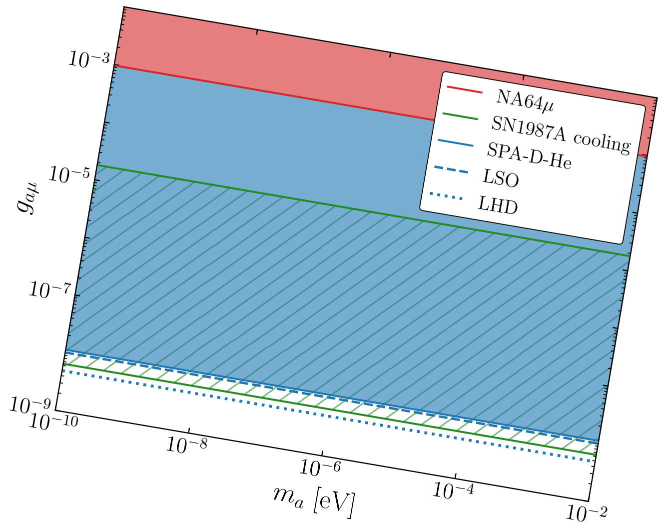

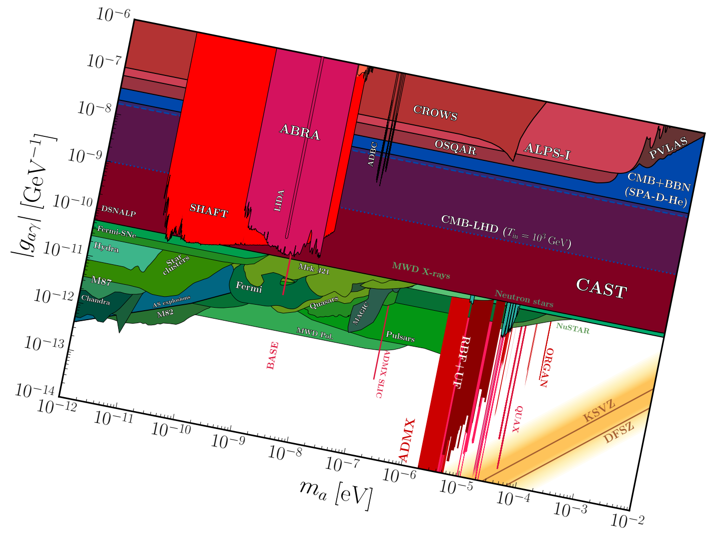

- Non-thermal spectral distortions induce shifts in ΔN_{eff}, with the magnitude of the effect depending on the specific production channel. The relevance of these differences for current and next-generation CMB experiments depends critically on the level of accuracy required in the analysis.

Prior sensitivity analysis

- Measure of the “distance” between two distributions

$$D_{\mathrm{KL}}(P \parallel Q) = \int \mathrm{d}x\, P(x) \log\left[\frac{P(x)}{Q(x)}\right]$$

- In the context of bayesian analysis it is used to asses the impact of different parameterisations by computing the information gain between the prior and the posterior.

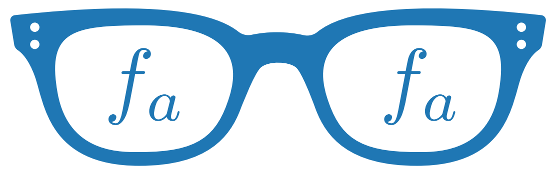

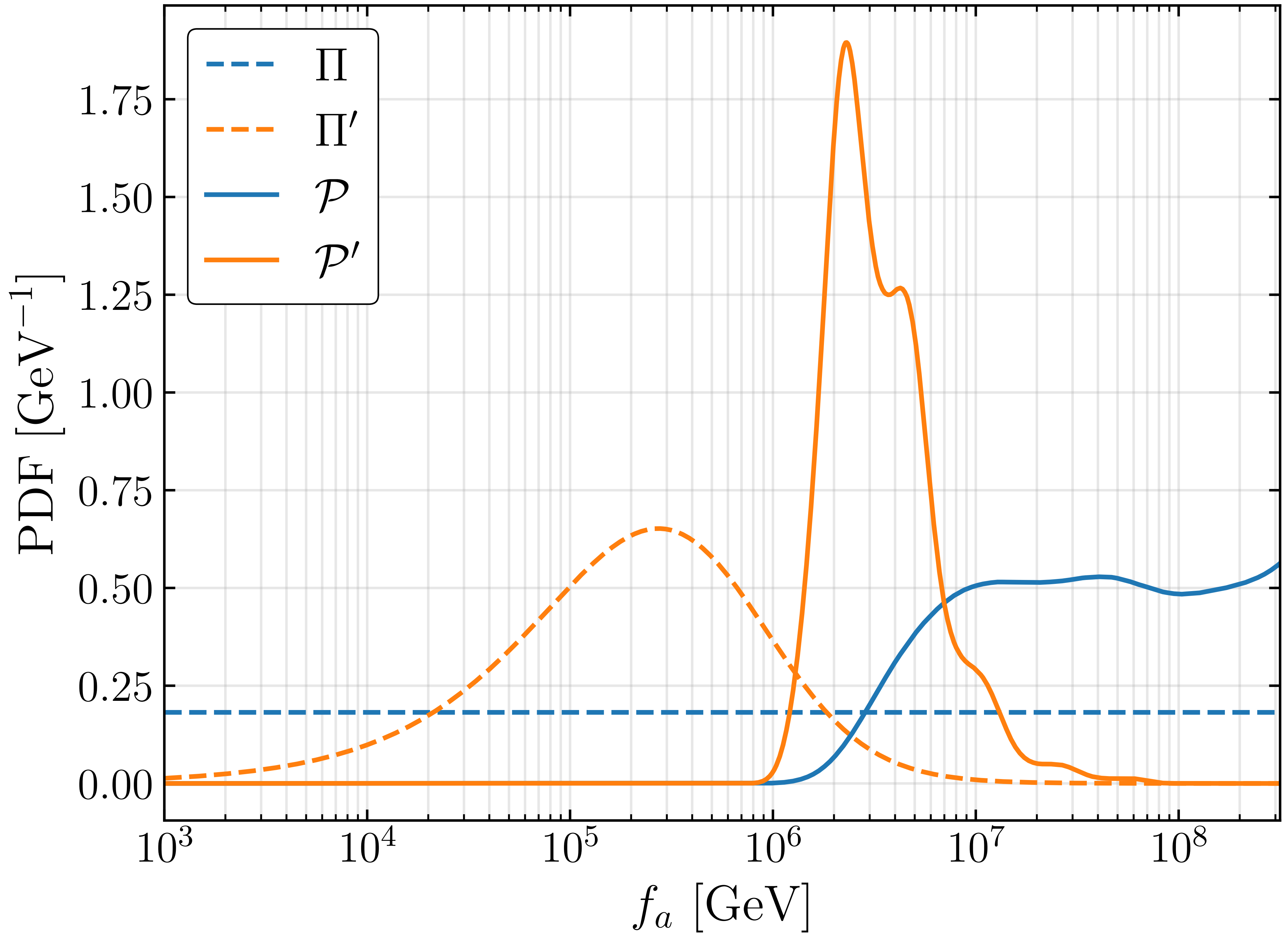

• Posterior

Flat prior on $\log_{10} f_a$ •

Prior sensitivity analysis

- Measure of the “distance” between two distributions

$$D_{\mathrm{KL}}(P \parallel Q) = \int \mathrm{d}x\, P(x) \log \left[\frac{P(x)}{Q(x)} \right]$$

- In the context of bayesian analysis it is used to asses the impact of different parameterisations by computing the information gain between the prior and the posterior.

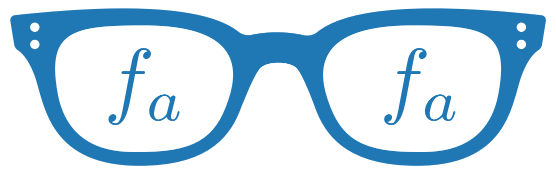

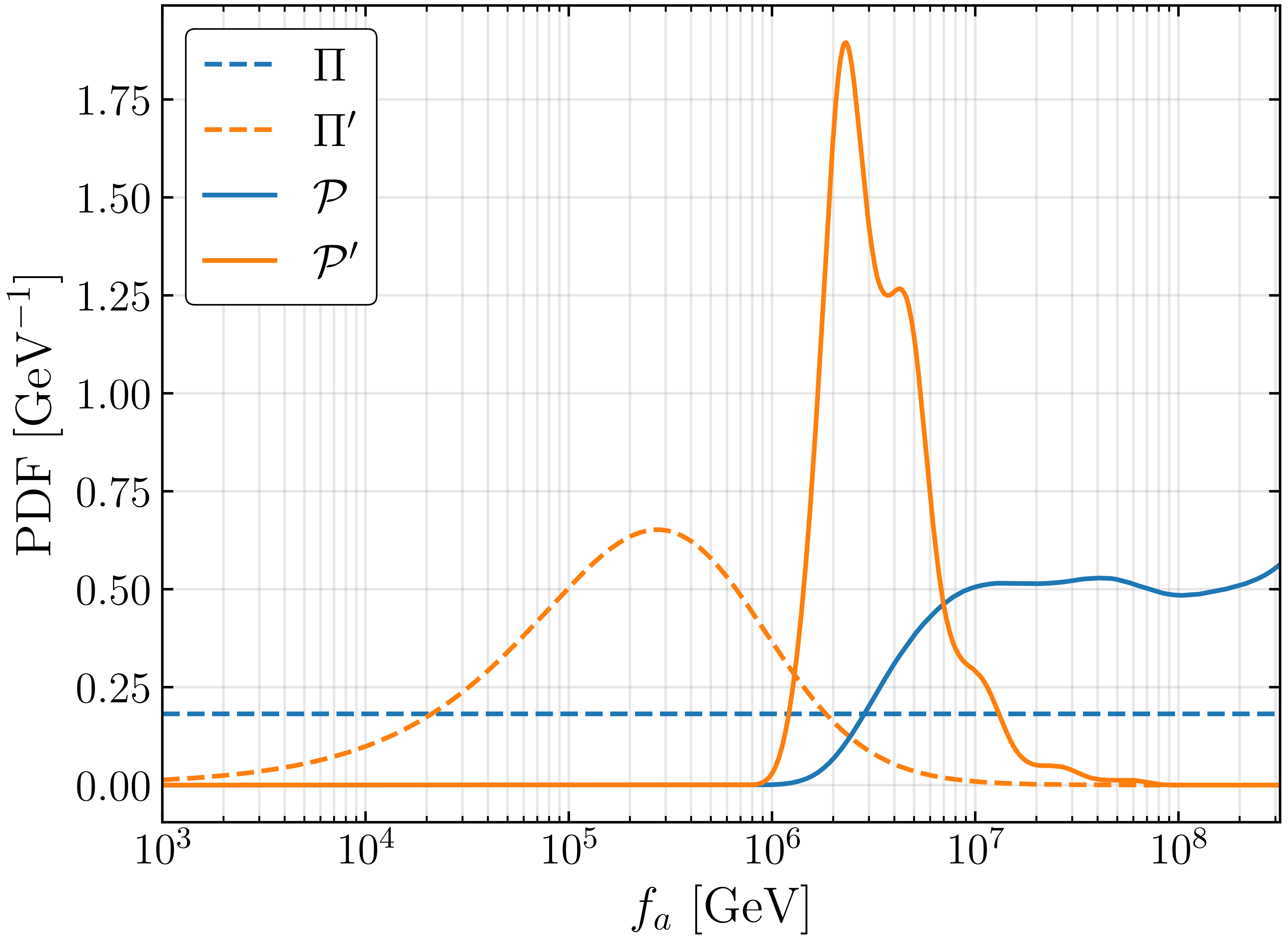

Posterior

Flat prior on $\log_{10} f_a$

$D_{\mathrm{KL}} = 0.94\,\mathrm{nat}$

Prior sensitivity analysis

- Measure of the "distance" between two distributions

$$D_{\mathrm{KL}}(P \parallel Q) = \int \mathrm{d}x\, P(x) \log\left[\frac{P(x)}{Q(x)}\right]$$

- In the context of bayesian analysis it is used to asses the impact of different parameterisations by computing the information gain between the prior and the posterior.

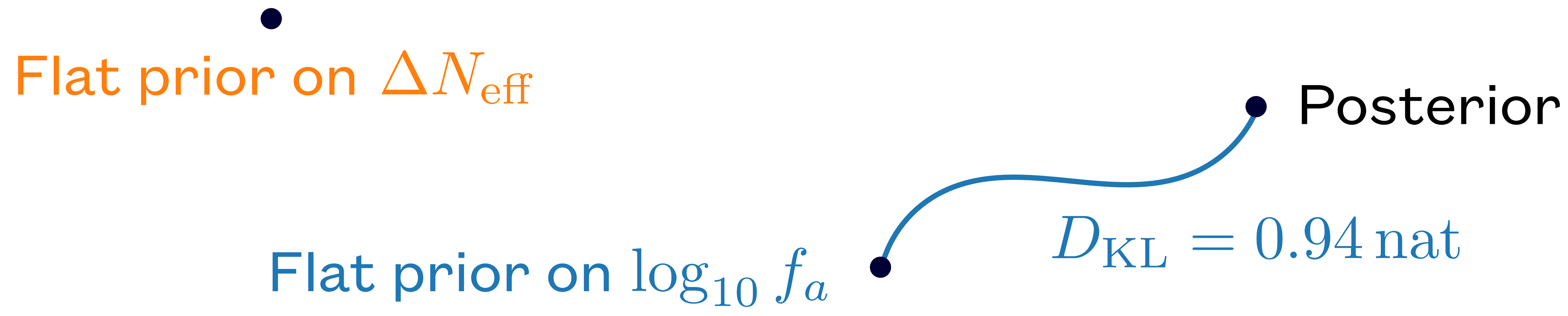

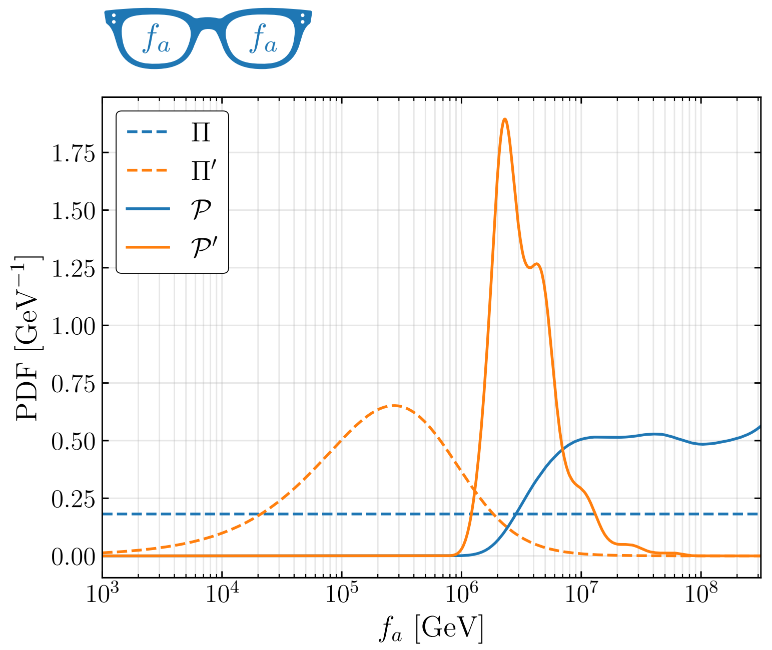

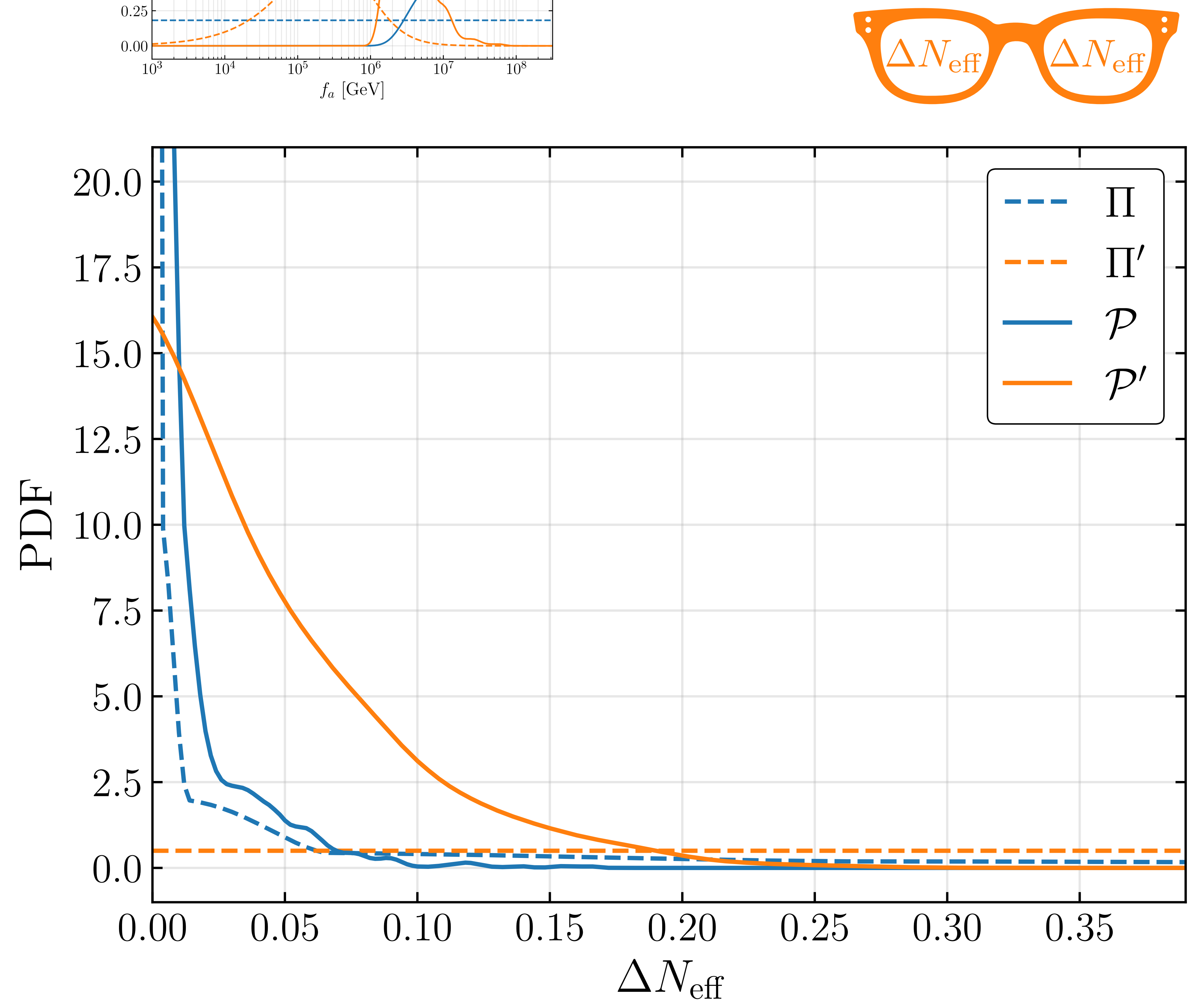

Prior sensitivity analysis

- Measure of the “distance” between two distributions

$$D_{\mathrm{KL}}(P \parallel Q) = \int \mathrm{d}x\, P(x) \log\left[\frac{P(x)}{Q(x)}\right]$$

- In the context of bayesian analysis it is used to asses the impact of different parameterisations by computing the information gain between the prior and the posterior.

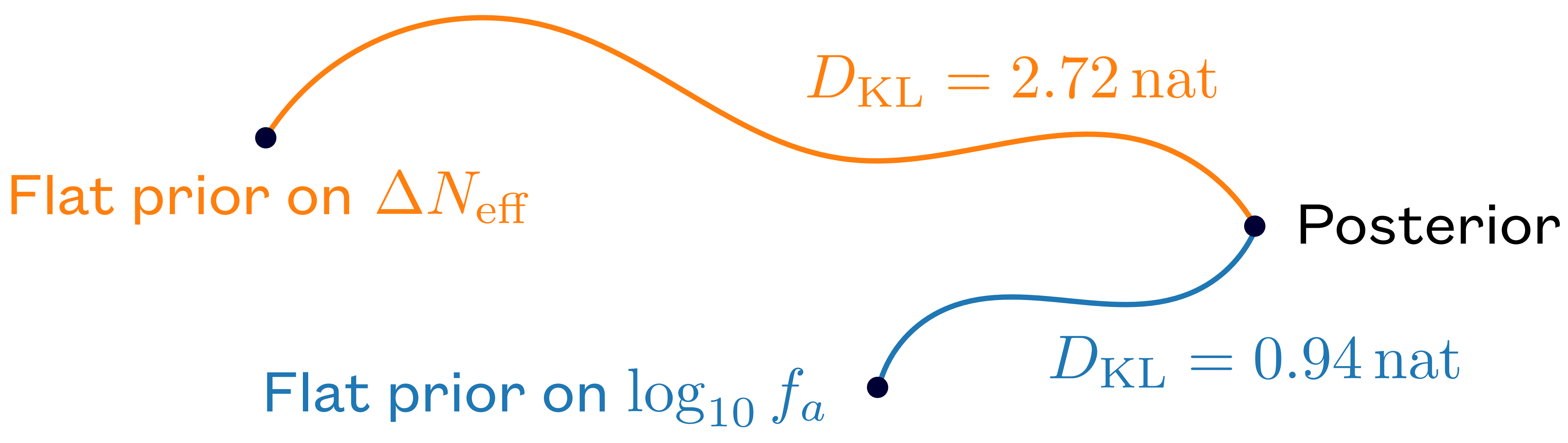

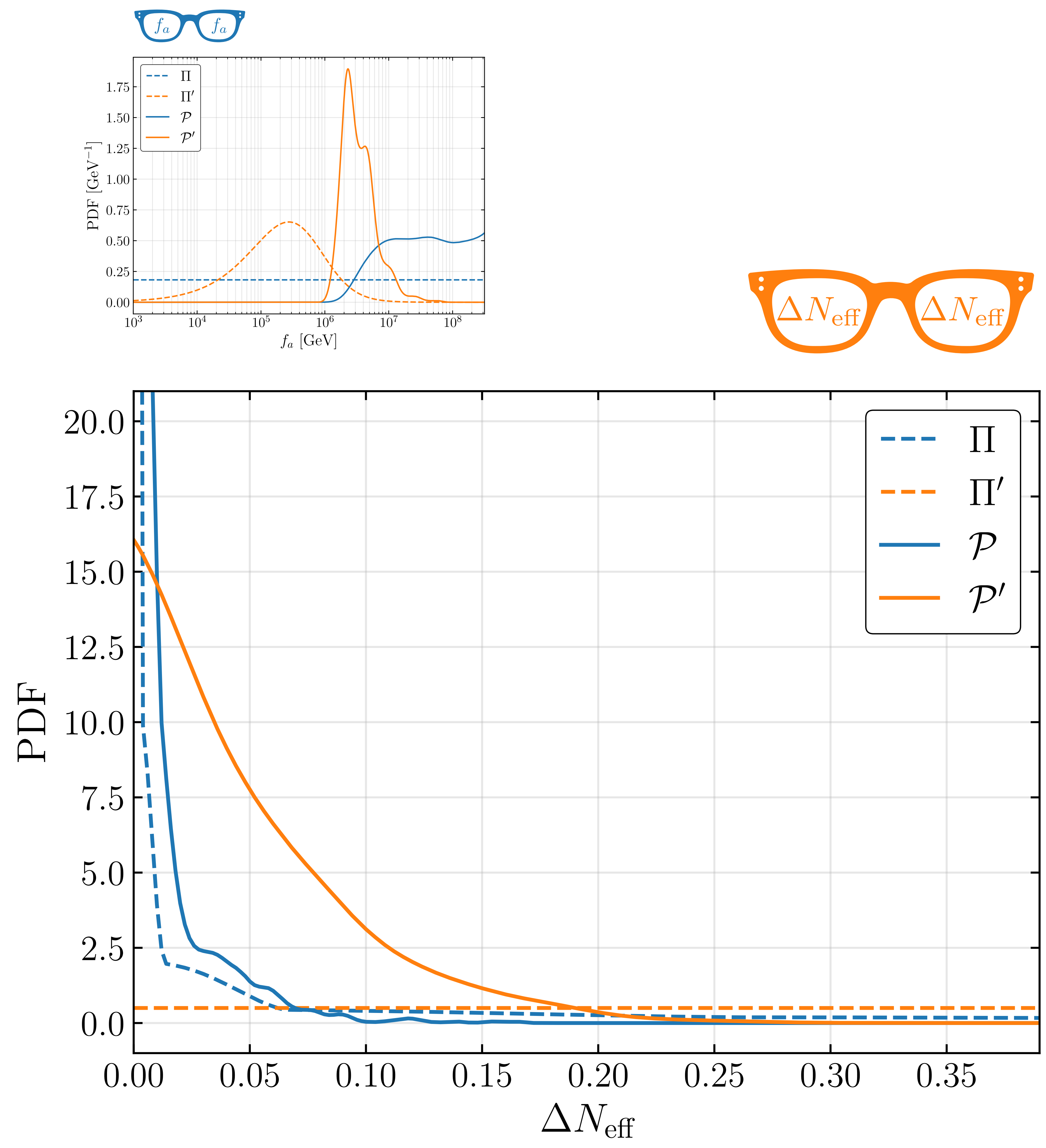

Impact of spectral distortions

- Small difference in constraints come from the direct effect of axion's PSD shape on CMB anisotropies. Neglecting those corrections introduce an error that we quantify through

$$\xi_i \equiv \frac{\Delta N_{\rm eff}^{95,\rm th} - \Delta N_{\rm eff}^{95,i}}{\Delta N_{\rm eff}^{95,i}}$$

where $i = \{e,\, \mu,\, \tau,\, \gamma\}$.

SPA-D-He

Model	ξ_i	$\sigma^i_{\rm MC}$	$[\xi_i - 3\sigma^i_{\rm MC},\, \xi_i + 3\sigma^i_{\rm MC}]$
e	-0.026	0.043	$[-0.103,\, 0.154]$
μ	0.019	0.049	$[-0.127,\, 0.165]$
τ	0.053	0.047	$[-0.087,\, 0.192]$
γ	0.032	0.043	$[-0.097,\, 0.161]$

LSO

Model	ξ_i	$\sigma^i_{\rm MC}$	$[\xi_i - 3\sigma^i_{\rm MC},\, \xi_i + 3\sigma^i_{\rm MC}]$
e	0.018	0.027	$[-0.061,\, 0.098]$
μ	-0.025	0.025	$[-0.098,\, 0.049]$
τ	-0.025	0.028	$[-0.109,\, 0.058]$
γ	-0.007	0.030	$[-0.096,\, 0.082]$

Impact of spectral distortions

- Small difference in constraints come from the direct effect of axion's PSD shape on CMB anisotropies. Neglecting those corrections introduce an error that we quantify through

$$\xi_i \equiv \frac{\Delta N_{\rm eff}^{95,{\rm th}} - \Delta N_{\rm eff}^{95,i}}{\Delta N_{\rm eff}^{95,i}}$$

  where $i = \{e, \mu, \tau, \gamma\}$.

- **Example:** We consider ALP-τ interactions tested with LSO like experiment.

  Replacing the exact PSD with is corresponding thermal approximation lead to a relative error of at most ~ 0.1 (at 99% CL)

SPA-D-He

Model	ξ_i	$\sigma^i_{\rm MC}$	$[\xi_i - 3\sigma^i_{\rm MC},\, \xi_i + 3\sigma^i_{\rm MC}]$
e	-0.026	0.043	$[-0.103,\, 0.154]$
μ	0.019	0.049	$[-0.127,\, 0.165]$
τ	0.053	0.047	$[-0.087,\, 0.192]$
γ	0.032	0.043	$[-0.097,\, 0.161]$

LSO

Model	ξ_i	$\sigma^i_{\rm MC}$	$[\xi_i - 3\sigma^i_{\rm MC},\, \xi_i + 3\sigma^i_{\rm MC}]$
e	0.018	0.027	$[-0.061,\, 0.098]$
μ	-0.025	0.025	$[-0.098,\, 0.049]$
τ	-0.025	0.028	$[-0.109,\, 0.058]$
γ	-0.007	0.030	$[-0.096,\, 0.082]$

Conclusions and future prospects

Conclusions and future prospects

1. Updated cosmological limits (and forecasts) on light ALPs coupled to photons and leptons.

Conclusions and future prospects

1. Updated cosmological limits (and forecasts) on light ALPs coupled to photons and leptons.

2. Development of a full flexible pipeline that allowed us to properly take into account distortions of ALPs PSD and to asses their impact on constraints.

Conclusions and future prospects

1. Updated cosmological limits (and forecasts) on light ALPs coupled to photons and leptons.

2. Development of a full flexible pipeline that allowed us to properly take into account distortions of ALPs PSD and to asses their impact on constraints.

3. Extension of the analysis to massive ALPs, where accounting for non-spectral distortions might be crucial.

Conclusions and future prospects

1. Updated cosmological limits (and forecasts) on light ALPs coupled to photons and leptons.
2. Development of a full flexible pipeline that allowed us to properly take into account distortions of ALPs PSD and to asses their impact on constraints.
3. Extension of the analysis to massive ALPs, where accounting for non-spectral distortions might be crucial.
4. Careful study of the gluon coupling case which requires new theoretical developments to be analysed at the sensitivity reached by current data.

Conclusions and future prospects

1. Updated cosmological limits (and forecasts) on light ALPs coupled to photons and leptons.

2. Development of a full flexible pipeline that allowed us to properly take into account distortions of ALPs PSD and to asses their impact on constraints.

3. Extension of the analysis to massive ALPs, where accounting for non-spectral distortions might be crucial.

4. Careful study of the gluon coupling case which requires new theoretical developments to be analysed at the sensitivity reached by current data.

Thank you!